CHAPTER (3)

3. Results and Discussion

The corrosion of metallic materials in acidic solutions caused damage to the national economy of the country. In order to reduce the corrosion of metals, several techniques have been applied. The use of inhibitors is one of the most practical methods for protection against corrosion in acidic media. Most well known acid inhibitors are organic compounds, such as those containing nitrogen, sulfur oxygen atoms [100,130]. To be effective, an inhibitor must also displace water from the metal surface; interact with anodic or cathodic reaction sites to retard the oxidation and reduction corrosion reaction, and to prevent transportation of water and corrosion-active species on the surface.

Corrosion process of carbon steel in acidic environments is very important scientific and technological topic in the oilfield industry. After desalting process, salts and sulphide compounds dissolved in crude can provoke the formation of a corrosive aqueous solution whose chemical composition involves the presence of both hydrochloric acid (HCl) and hydrogen sulfide (H_2S). This solution is very aggressive causing varied damages on carbon steel surface during plant operation [131].

Perusals of the literature on acid corrosion inhibitors act by adsorption on the metal surface. This phenomenon could take place via (i) electrostatic attraction between the charged metal and the charged inhibitor molecules (ii) dipole-type interaction between uncharged electron pairs in the inhibitor with the metal, (iii) π electron-interaction with the metal, and (iv) a combination of all of the above. The compounds containing nitrogen can provide excellent inhibition in acidic media [132].

The results obtain from experiments described in chapter (2) are presented in this chapter.

Cationic gemini surfactants were selected as corrosion inhibitors for C-steel in 1M hydrochloric acid solutions. The effect of inhibitor concentration was studied, as described in chapter (2), by weight loss method, potentiodynamic polarization and by electrochemical impedance spectroscopy (EIS) and mechanism of inhibition. Weight loss method was carried at different temperatures (30, 40, 50, and 60±1°C) and all electrochemical techniques were carried out at 30±1°C. The effect of 1M hydrochloric acid on corrosion rate was studied, and then the inhibition efficiency was determined in presence of different concentrations of cationic gemini surfactants, (compound I, compound II, and compound III).

3.1 Synthesis of inhibitors

Reaction of different alkyl bromide with p-N,N-dimethylamino-benzaldehyde, then react with 1,4-diaminebenzene to obtain different inhibitors compounds I, II and III represent in schematics (3:1-3:3).

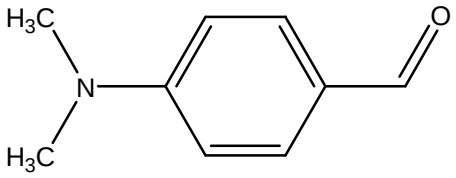

+ $CH_3(CH_2)_6CH_2Br$

p-N,N-dimethylaminobenzaldehyde

octylbromide

reflux
ethanol

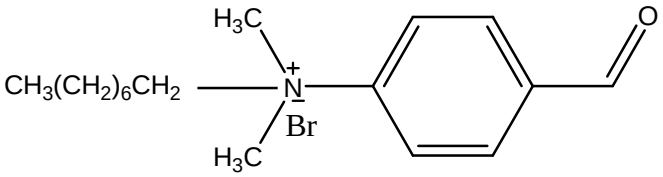

p-N,N,N-octyldimethylammonium bromide benzaldehyde

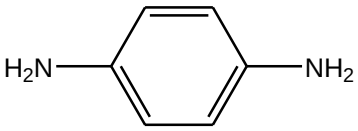

Benzene-1, 4-diamine

reflux
ethanol

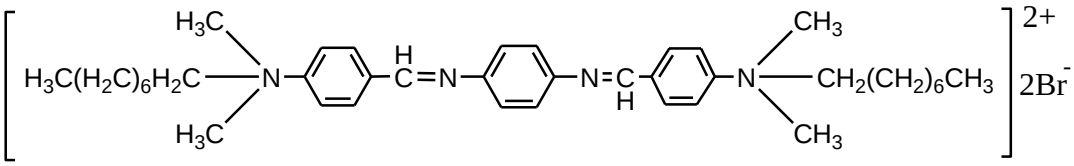

bis(p-(N,N,N-octyldimethylammonium bromide)benzylidene)benzene-1,4-diamine

Scheme (3:1): Preparation of compound I.

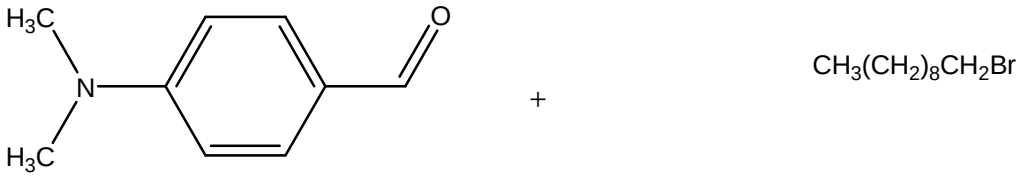

p-N,N-dimethylaminobenzaldehyde

decylbromide

reflux
ethanol

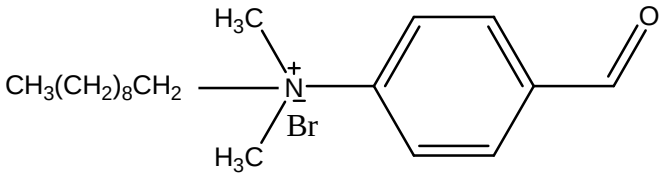

p-N,N,N-decyldimethylammonium bromide benzaldehyde

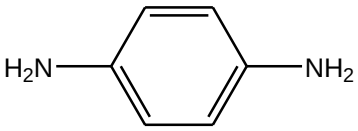

Benzene-1, 4-diamine

reflux
ethanol

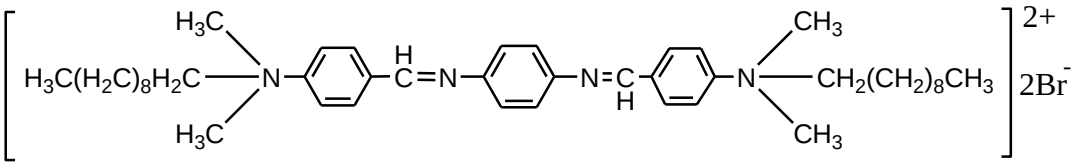

bis(p-(N,N,N-decyldimethylammonium bromide)benzylidene)benzene-1,4-diamine

Scheme (3:2): Preparation of compound II.

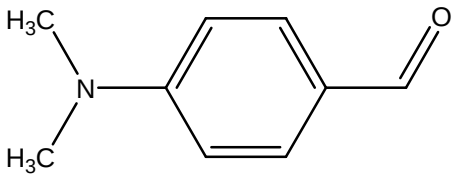

+ $CH_3(CH_2)_{10}CH_2Br$

p-N,N-dimethylaminobenzaldehyde

dodecylbromide

reflux
ethanol

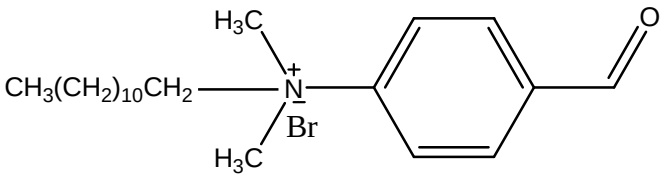

p-N,N,N-dodecyldimethylammonium bromide benzaldehyde

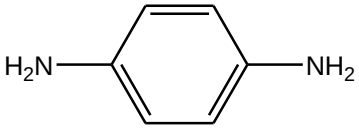

Benzene-1, 4-diamine

reflux
ethanol

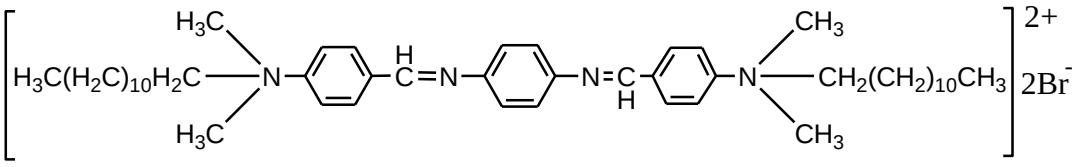

bis(p-(N,N,N-dodecyldimethylammonium bromide)benzylidene)benzene-1,4-diamine

Scheme (3:3): Preparation of compound III.

3.2 Characterization of the synthesized surfactants

The chemical structures of the prepared surfactants were confirmed by the FTIR and ^{1}HNMR spectra as shown in Fig. (3:1-3:6).

3.2.1. FTIR spectroscopy

FTIR spectra of the synthesized compounds showed the following absorption bands at 716.85cm^{-1} (CH_2 rocking), 1366.75 cm^{-1} (CH_2 deformation), 2914.63-2846.78 cm^{-1} (CH_2 stretching), 3177.47, 1062.77 cm^{-1} (C-N^{+}), 1652.31 cm^{-1} (C=N) and 812.73, 1535 cm^{-1} (C=C). The FTIR spectra confirmed the expected function groups in the synthesized cationic gemini surfactants.

3.2.2. ^{1}HNMR spectroscopy

The ^{1}H-NMR spectra of the synthesized compounds showed different bands at δ=0.90 ppm (t, 3H, $NCH_2(CH_2)_nCH_2C\underline{\mathbf{H}}_3$); δ=1.33 ppm (m, 4H, $NCH_2(CH_2)_nC\underline{\mathbf{H}}_2CH_3$); δ=1.29 ppm (m, 5H, $NCH_2(C\underline{\mathbf{H}}_2)_nCH_2CH_3$); δ=1.73 ppm (t, 3H, $NC\underline{\mathbf{H}}_2(CH_2)_nCH_2CH_3$); δ=3.29 ppm (s, 1H, $NC\underline{\mathbf{H}}_3$); δ=7.64 ppm (d, 2H, o-bezelidine nucleus); δ=7.75 ppm (d, 2H, m- bezelidine nucleus); δ=9.64 ppm (s, 1H, N=C**H**); δ=6.74 ppm (d, 2H, o,m-phenylidine nucleus). The data of ^{1}HNMR spectra confirmed the expected hydrogen proton distribution in the synthesized cationic gemini surfactants.

All prepared cationic gemini surfactants have the same signals. The only difference between the signals of these compounds is the signal intensity of methylene proton (m, 6H, NCH_2 $(C\underline{\mathbf{H}}_2)_n$ CH_2CH_3), where the intensity of this signal increases by increasing the methylene groups (chain length) of the prepared compounds.

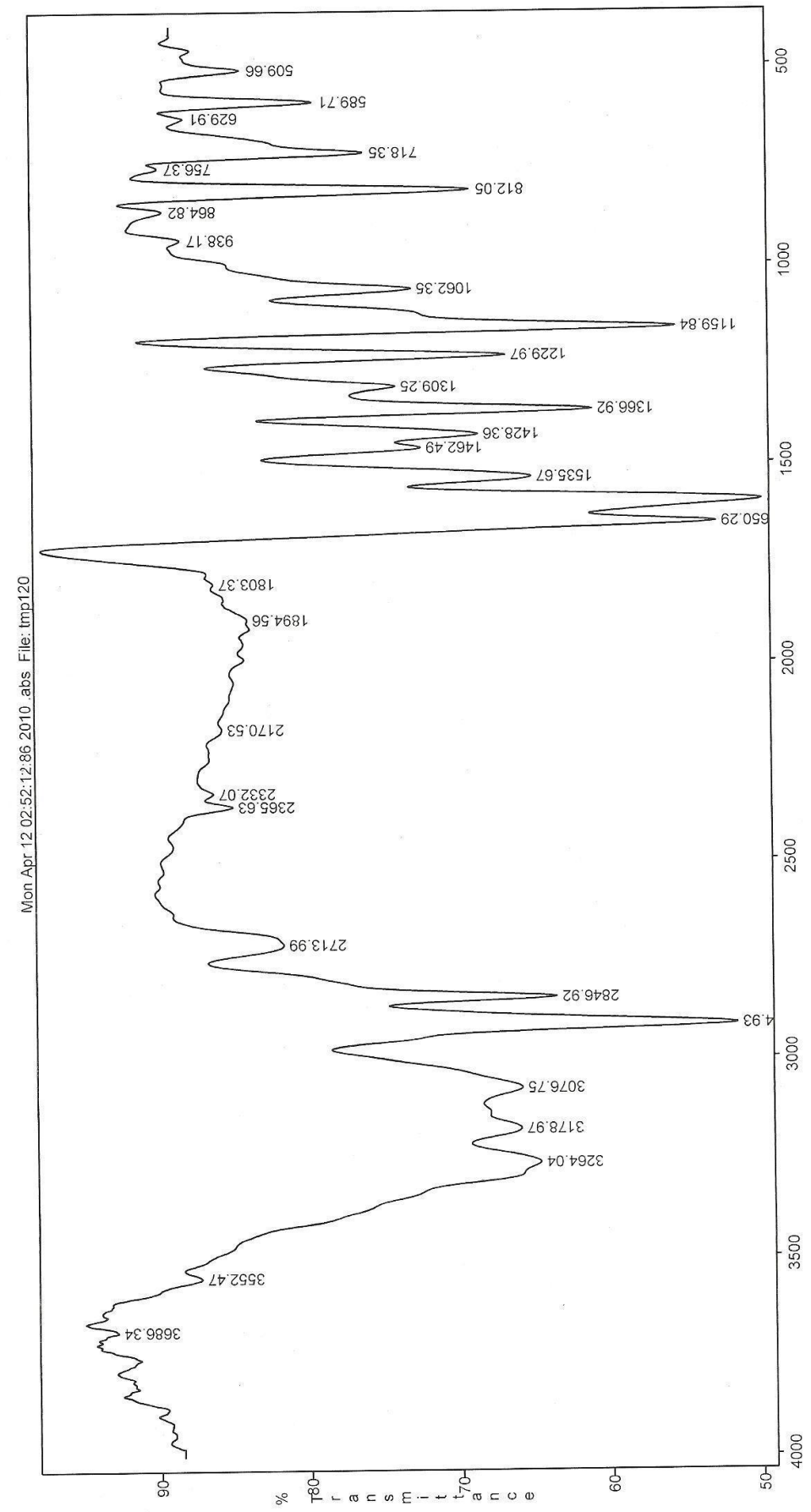

Fig. (3:1): FTIR of compound I.

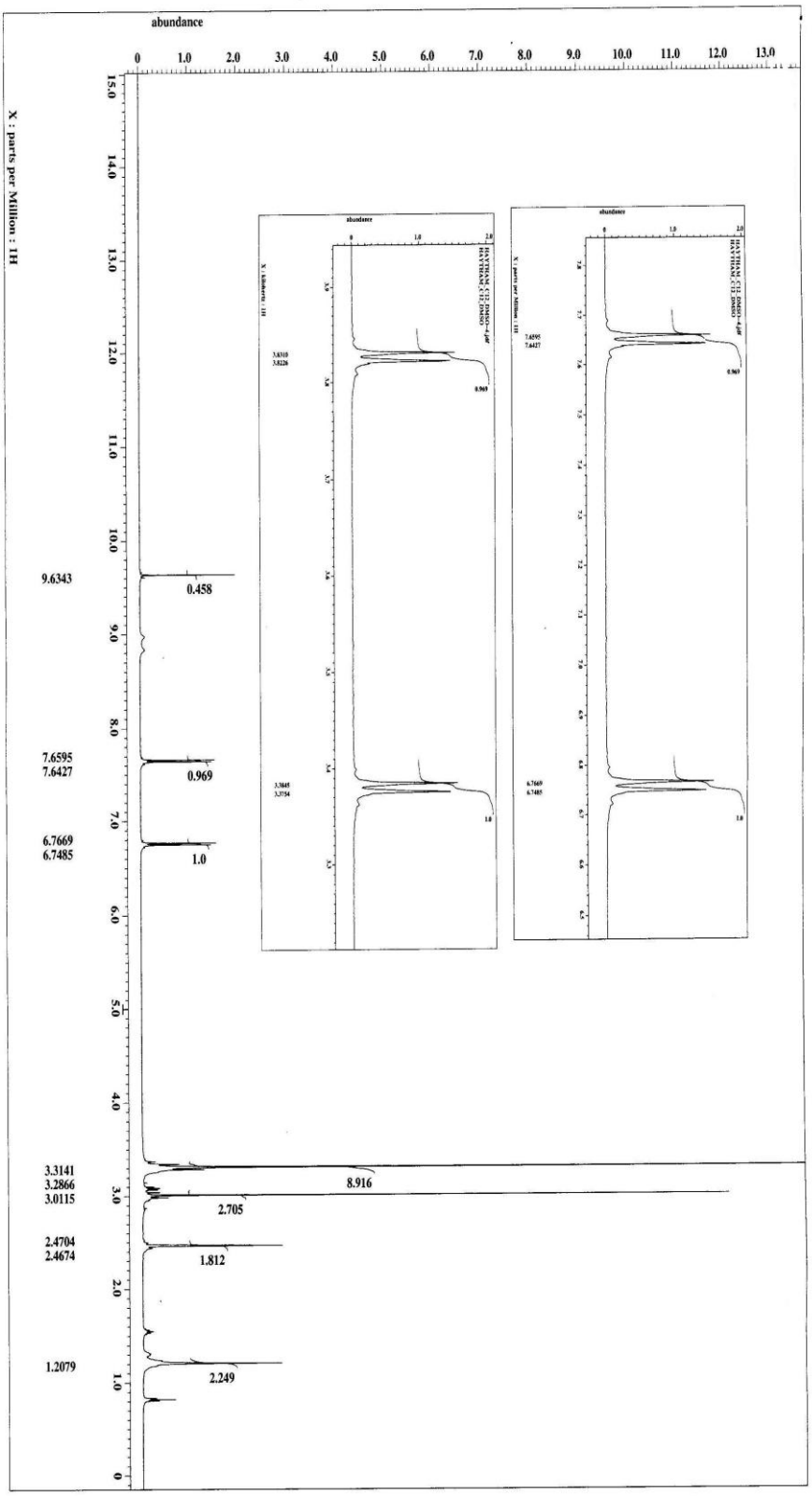

Fig. (3:2): ^{1}HNMR of compound I.

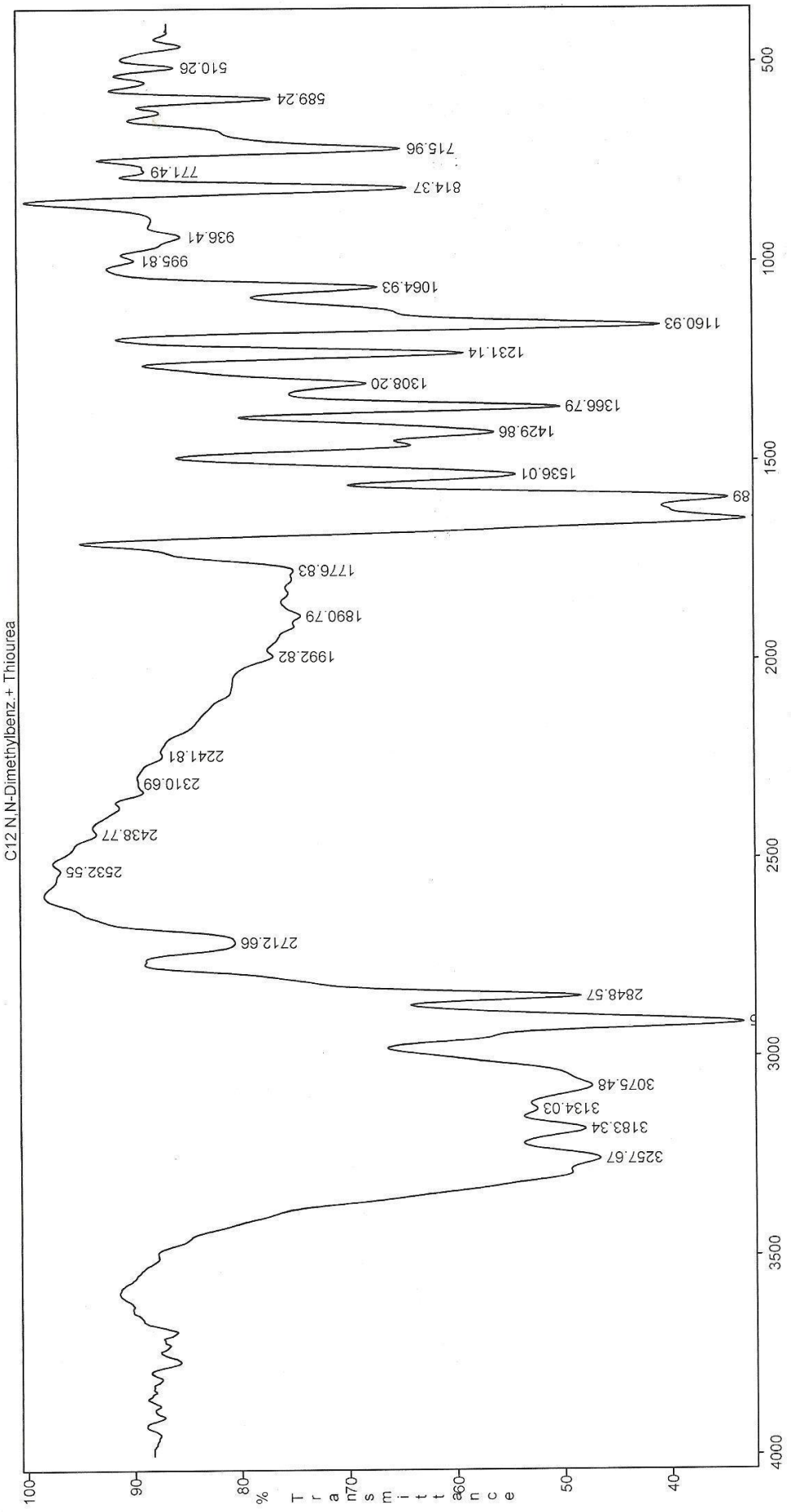

Fig. (3:6): FTIR of compound II.

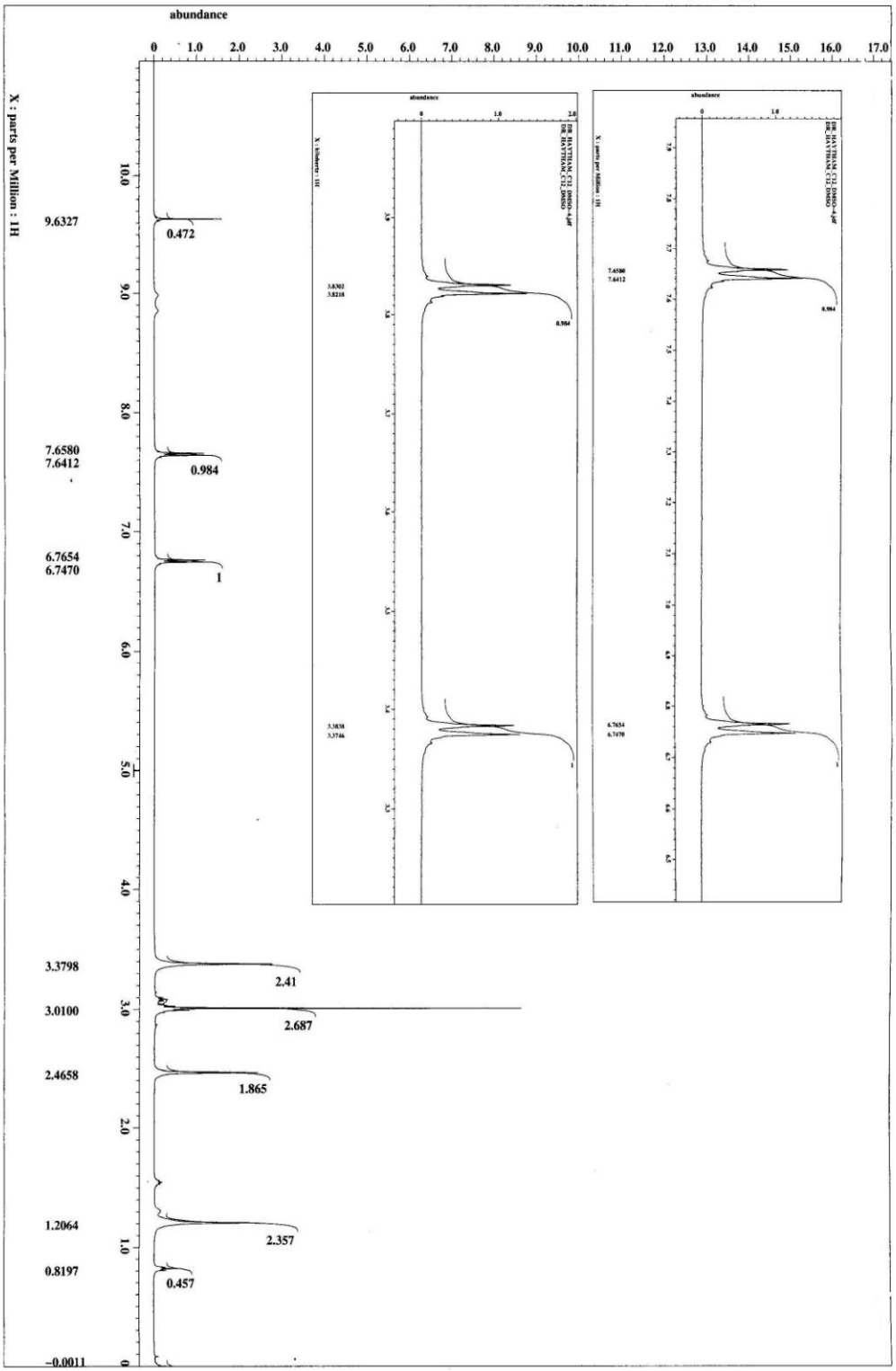

Fig. (3:4): 1HNMR of compound II.

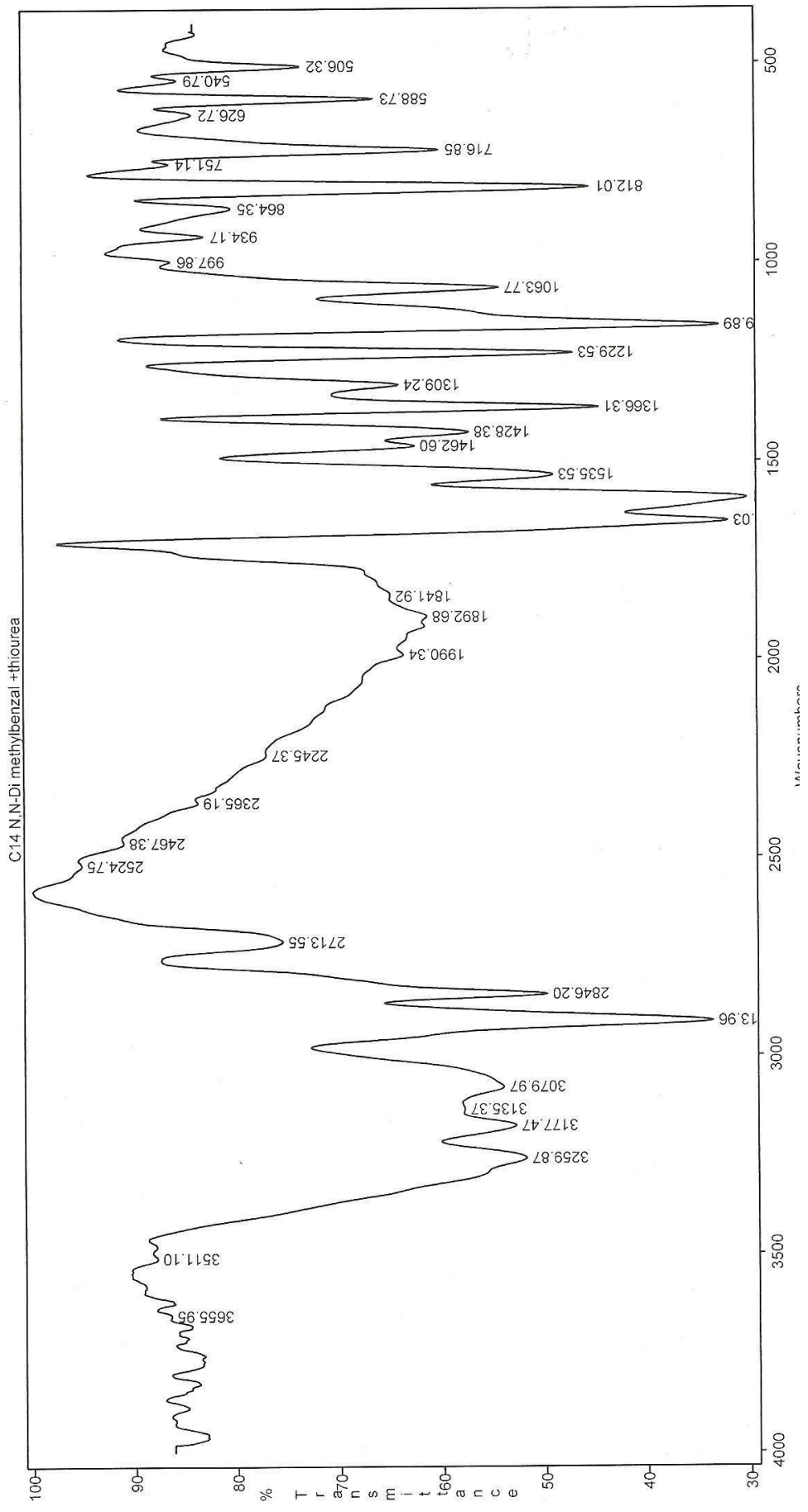

Fig. (3:5): FTIR of compound III.

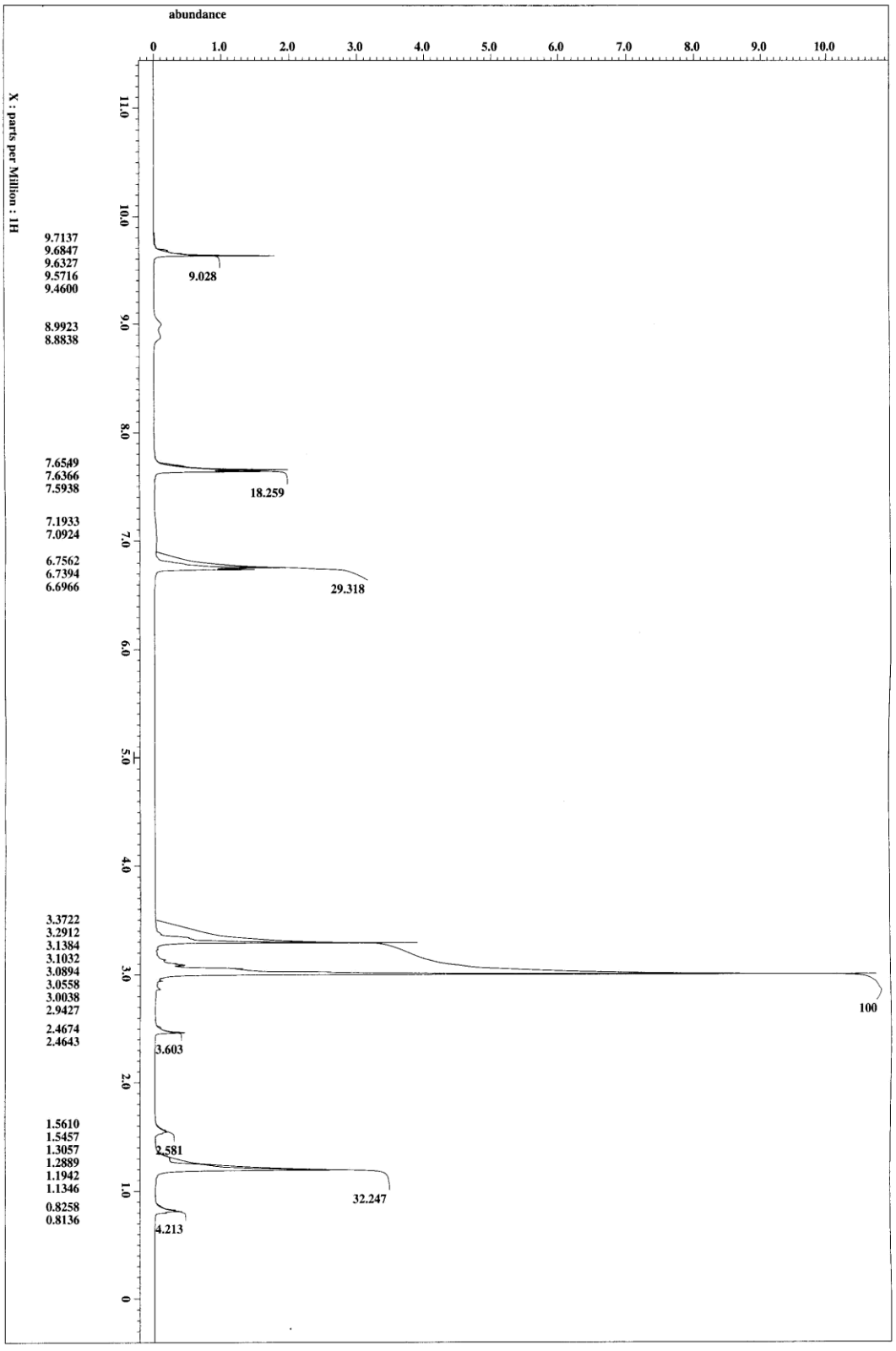

Fig. (3:6): ^{1}HNMR of compound III.

Studying the corrosion inhibition of C-steel in hydrochloric acid by new cationic gemini surfactants

3.3 Weight loss measurements

3.3.1 Effect of inhibitor concentrations

The inhibiting effect of cationic gemini surfactants, for corrosion of C-steel in 1M HCl solution was studied using weight loss method. Weight loss of C-steel in mg. was calculated after fixed time 24 hours in absence and presence of different concentrations of cationic gemini surfactants. Fig. (3:7) represents the relation between the values of percentage inhibition efficiency with logarithmic the concentration of the synthesized cationic gemini surfactants. Inspection of this Fig. reveals that, the values of percentage inhibition efficiency increases with increasing the concentration of these cationic gemini surfactants depending on the nature of substitution.

In all cases the increase in inhibitor concentration was accompanied by a decrease in weight loss and an increase in the percentage inhibition. These results lead to conclusion that, the compounds under investigation are fairly efficient as an inhibitors for C-steel dissolution in hydrochloric acid solution. To clear up the influence of these inhibitors on the mechanism of inhibition, the corrosion rate (k) was calculated using the following equation:

$$k = (W_{free} - W_{inh)} / At \qquad (3.2)$$

where, k is the corrosion rate, W_{inh} and W_{free} are the weights loss of specimen in presence and absence of inhibitor, respectively, A is the surface area in cm^2 and t is the time in hours.

The degree of surface coverage (Θ) by the adsorbed compounds was calculated from equation:

$$\Theta = (W_{free} - W_{inh}) / W_{free} \qquad (3.1)$$

It was found that the degree of surface coverage (Θ) of the inhibitor increases by increasing the inhibitor concentration. The inhibition efficiencies (η_w %) of cationic gemini surfactants, were determined from equation [133, 134] :-

$$\eta_{w\,\%} = (\Theta) \times 100 \qquad (3.3)$$

from the calculated values of ($\boldsymbol{\eta_w}$ %) which are given in Table (3:1-3:3) the order of the inhibition efficiencies of cationic gemini surfactants, decrease in the following arrangement:

compound III >compound II > compound I

This order will be discussed later.

3.3.2 Effect of temperature

The effect of rising temperature has a great important to study the corrosion of C-steel in hydrochloric acid solution and its inhibition. The inhibition efficiency of different inhibitors is very important in elucidation of the mechanism and kinetic of their action and ultimately, showing the proper selection of these inhibitors for specific practical situations.

In this part, the effect of rising temperature on both corrosion and corrosion inhibition of C-steel in 1M HCl solution at different temperatures was studied in range (30-60°C) and this investigated by weight loss measurements. Weight loss of C-steel in mg. was determined after fixed time 24 hours in absence and presence of different concentrations of cationic gemini surfactants, at different temperatures.

Figs. (3:8-3:10) represent the effect of rising temperature on the inhibition efficiency obtained by weight loss method at different concentrations of compounds I, II and III, respectively. The corrosion

parameters such as weight loss (Δ W), rate of corrosion (k), surface coverage (Θ) and inhibition efficiency (η_w) for compound I, II and III are listed in Tables (3:1-3:3), respectively.

Inspection of Tables (3:1-3:3) shows that by increasing the temperature, the corrosion rate increases rapidly in absence of inhibitor and in the presence of inhibitors also, the corrosion rate increases, in range (30-40°C), and decreases again in range (40-60°C), these compounds are efficient inhibitors in the temperature range (30-60°C).

The temperature range (30-40°C) has a reverse relationship with the percentage inhibition efficiency and by increasing temperature range (40- 60°C) increasing the percentage inhibition efficiency, this means that adsorption of cationic gemini surfactants, on the metal surface is mixed between physical and chemical adsorption.

Further inspection of Tables (3:1-3:3) reveals that the percentage inhibition efficiency is decreased with the temperature range (30-40°C), this behavior can be explained on the basis that the behavior of inhibitors in this range leads to desorption of the adsorbed compounds of the inhibitor from the metal surface (weak adsorption of the inhibitors molecules) physical adsorption, and by increasing temperature in range (40-60°C) show the percentage inhibition efficiency is increased in this range of temperature, this behavior can be explain on the basis that the increase of the temperature in range (40-60°C) leads to strong adsorption (chemical adsorption) of the inhibitors molecules on the metal surface. With increasing the temperature, some chemical changes occur in the inhibitor molecules, leading to an increase in the electron densities at the adsorption centers of the molecule, causing an improvement in inhibitor efficiency [135, 136].

From the obtained results we can say that the adsorption of inhibitor on the carbon steel surface is physical-chemical adsorption.

The S-shape of the adsorption Figs. (3:7-3:10) reflects three different modes of adsorption:

(1) At low concentrations, it seems that the adsorption takes place by horizontal binding to hydrophobic region Fig. (11a). This adsorption is favoured by an electrostatic interaction between the two ammonium groups (N^+) and cathodic sites on the one hand and Br^- ion on the metallic surface on the other hand.

(2) When the inhibitor concentration increases, a perpendicular adsorption takes place as a result of an inter-hydrophobic chain interaction Fig. (11b).

(3) At higher inhibition concentrations, an efficiency plateau appears. As we have shown from electrochemical impedance, there is one capacitive loop at high frequencies which some authors [137,139] attributed to the formation of a bimolecular layer on the iron surface Fig. (11c).

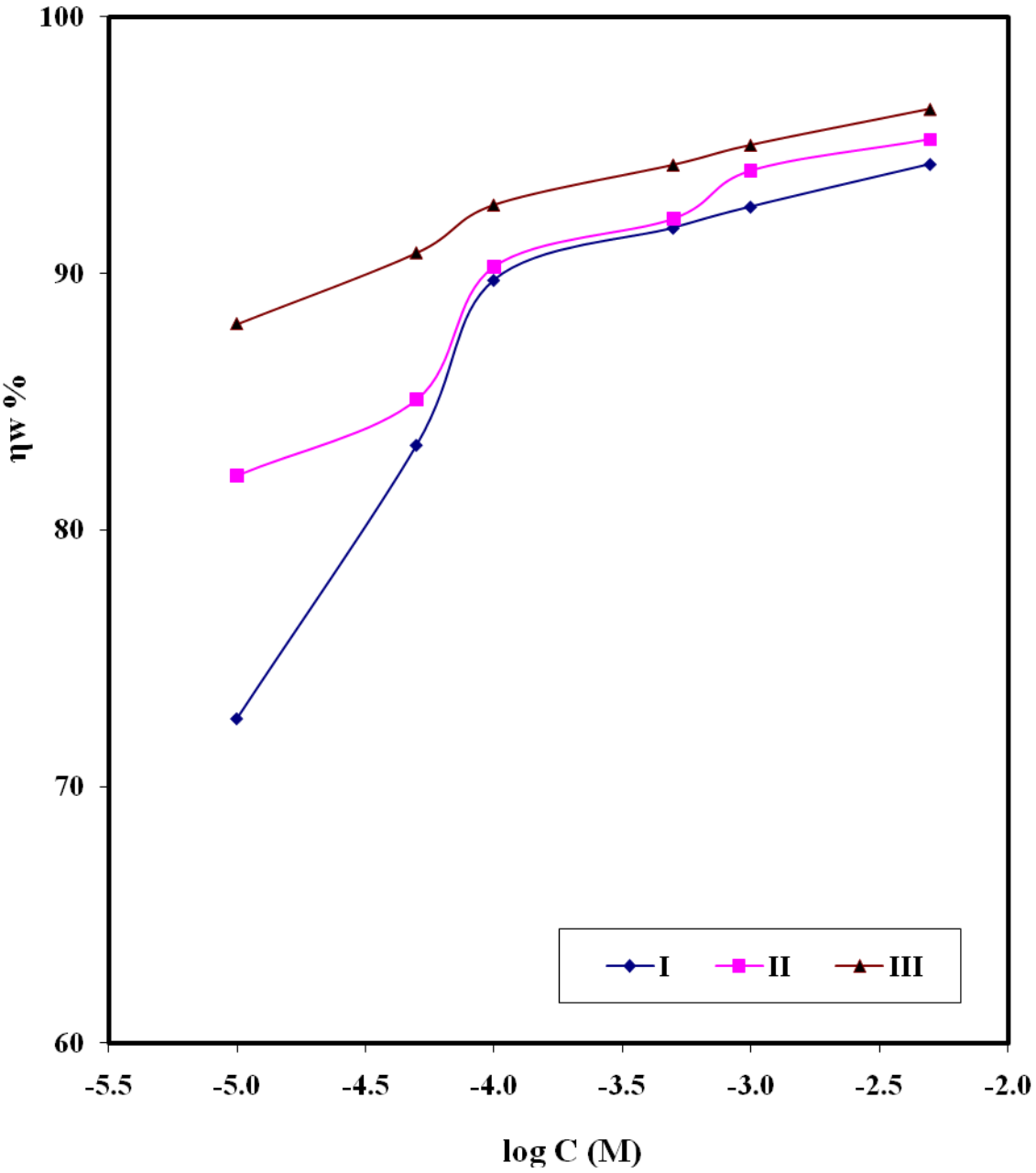

Fig. (3:7): The variation of the inhibition efficiency obtained by weight loss method versus log (C) of cationic gemini surfactants in 1M HCl solution at 30^{o}C.

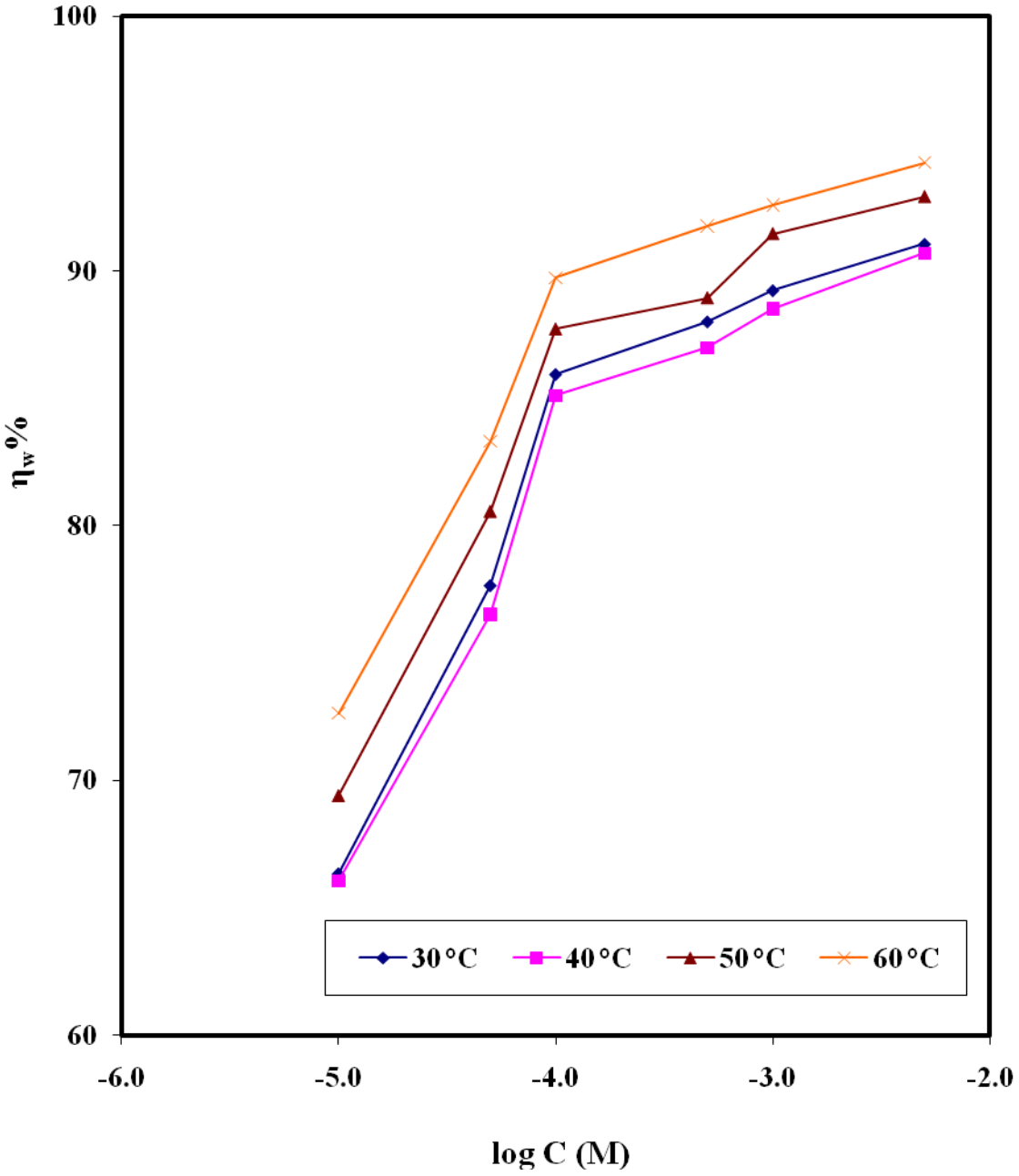

Fig. (3:8): Effect of temperature on the inhibition efficiency obtained by weight loss method for carbon steel in 1M HCl in presence of different concentrations of compound I.

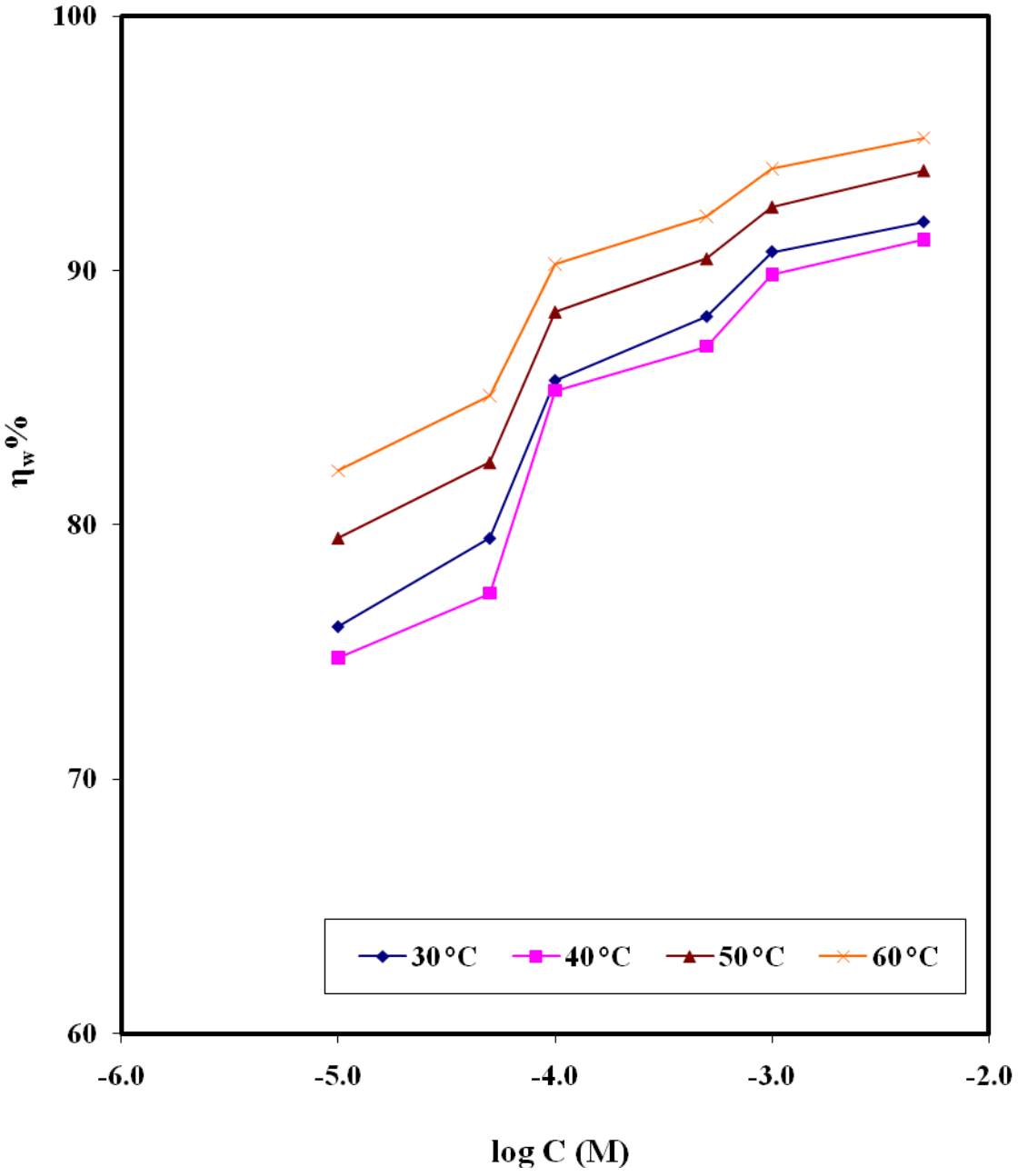

Fig. (3:9): Effect of temperature on the inhibition efficiency obtained by weight loss method for carbon steel in 1M HCl in presence of different concentrations of compound II.

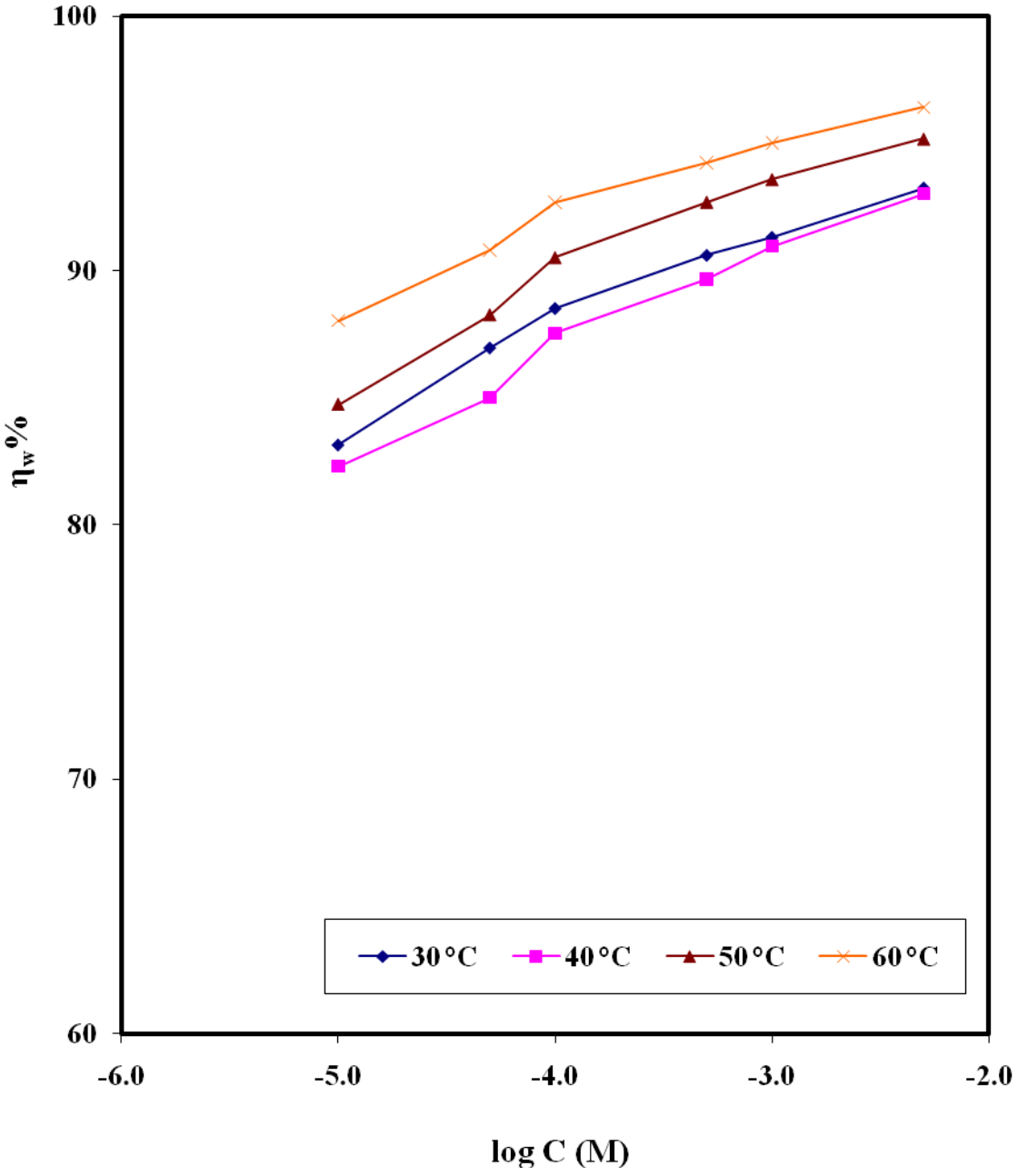

Fig. (3:10): Effect of temperature on the inhibition efficiency obtained by weight loss method for carbon steel in 1M HCl in presence of different concentrations of compound III.

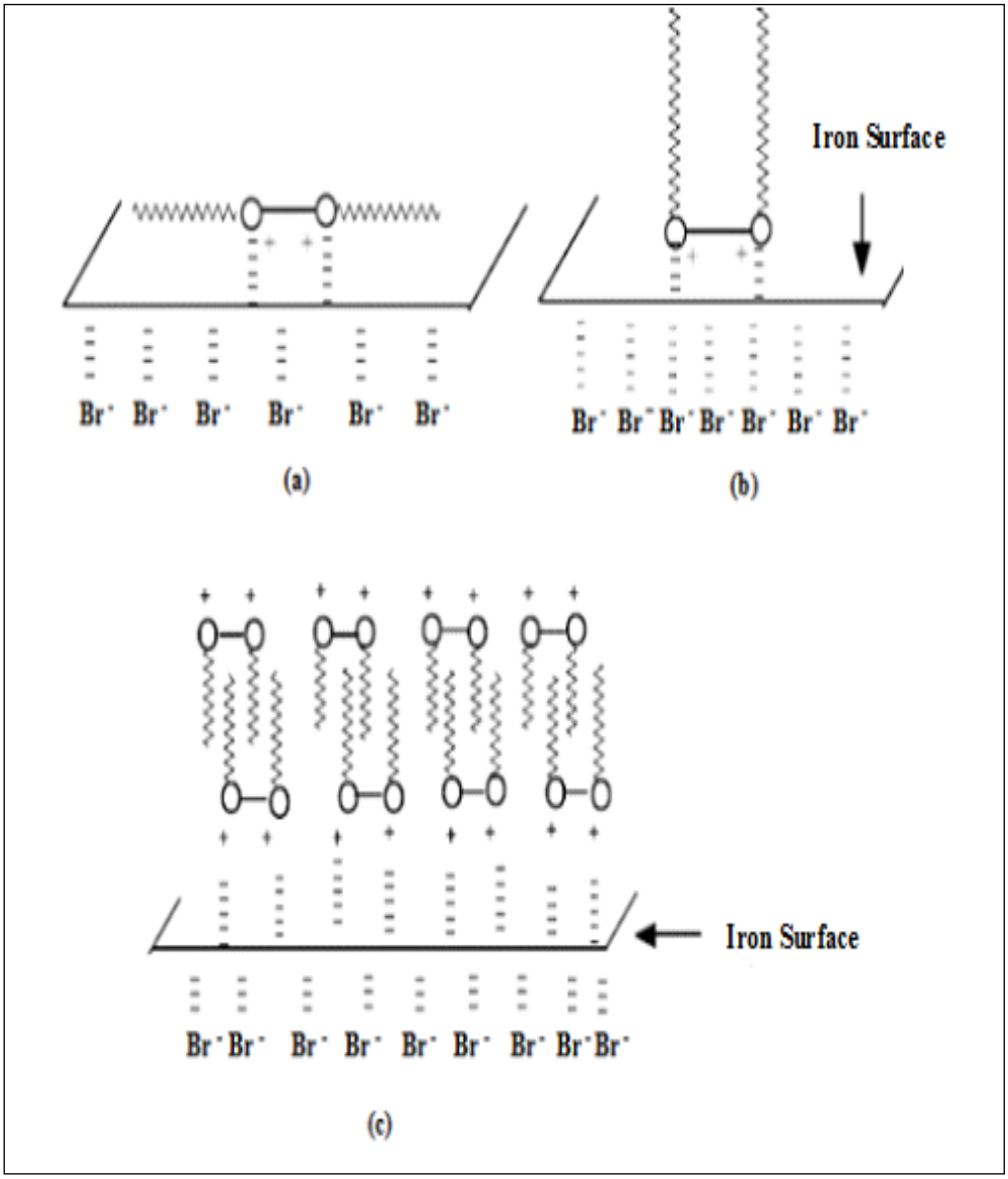

Fig. (3:11): Mode of adsorption of the synthesized cationic gemini surfactants on the carbon steel surface in 1 M HCl solution.

Table (3:1): Corrosion rate of carbon steel, surface coverage and percentage inhibition efficiency for carbon steel in 1M HCl in the absence and presence of different concentrations of compound I from weight loss measurements at different temperatures.

Temp. °C	Conc. of inhibitor M	Weight loss (mg)	k $mg/cm^2.h$	Θ	η_w %
30	0.00	0.5224	0.3922	-	-
	$1x10^{-5}$	0.1758	0.2602	0.66	66.35
	$5x10^{-5}$	0.1167	0.3047	0.78	77.66
	$1x10^{-4}$	0.0734	0.3372	0.86	85.95
	$5x10^{-4}$	0.0626	0.3454	0.88	88.02
	$1x10^{-3}$	0.0562	0.3503	0.89	89.24
	$5x10^{-3}$	0.0467	0.3575	0.91	91.06
40	0.00	0.8816	0.6619	-	-
	$1x10^{-5}$	0.2992	0.4372	0.66	66.06
	$5x10^{-5}$	0.2070	0.5065	0.77	76.52
	$1x10^{-4}$	0.1313	0.5634	0.85	85.11
	$5x10^{-4}$	0.1147	0.576	0.87	86.99
	$1x10^{-3}$	0.1012	0.5862	0.89	88.52
	$5x10^{-3}$	0.0820	0.6007	0.91	90.70
50	0.00	1.6789	1.2604	-	-
	$1x10^{-5}$	0.5133	0.8751	0.69	69.43
	$5x10^{-5}$	0.3262	1.0156	0.81	80.57
	$1x10^{-4}$	0.2061	1.1059	0.88	87.72
	$5x10^{-4}$	0.1855	1.1214	0.89	88.95
	$1x10^{-3}$	0.1433	1.1532	0.91	91.46
	$5x10^{-3}$	0.1189	1.1715	0.93	92.92
60	0.00	2.9378	2.2056	-	-
	$1x10^{-5}$	0.8036	1.6023	0.73	72.65
	$5x10^{-5}$	0.4903	1.8375	0.83	83.31
	$1x10^{-4}$	0.3014	1.9794	0.90	89.74
	$5x10^{-4}$	0.2416	2.0244	0.92	91.78
	$1x10^{-3}$	0.2174	2.0426	0.93	92.60
	$5x10^{-3}$	0.1686	2.0794	0.94	94.26

Table (3:2): Corrosion rate of carbon steel, surface coverage and percentage inhibition efficiency for carbon steel in 1M HCl in the absence and presence of different concentrations of compound II from weight loss measurements at different temperatures.

Temp. °C	Conc. of inhibitor M	Weight loss (mg)	k $mg/cm^2.h$	Θ	η_w %
30	0.00	0.5224	0.3922	-	-
	$1x10^{-5}$	0.1253	0.2981	0.76	76.01
	$5x10^{-5}$	0.1072	0.3118	0.79	79.48
	$1x10^{-4}$	0.0748	0.3362	0.86	85.68
	$5x10^{-4}$	0.0617	0.3461	0.88	88.19
	$1x10^{-3}$	0.0484	0.3562	0.91	90.74
	$5x10^{-3}$	0.0423	0.3608	0.92	91.90
40	0.00	0.8816	0.6619	-	-
	$1x10^{-5}$	0.2223	0.495	0.75	74.78
	$5x10^{-5}$	0.2000	0.5118	0.77	77.31
	$1x10^{-4}$	0.1298	0.5646	0.85	85.28
	$5x10^{-4}$	0.1144	0.5762	0.87	87.02
	$1x10^{-3}$	0.0896	0.5949	0.90	89.84
	$5x10^{-3}$	0.0775	0.6041	0.91	91.21
50	0.00	1.6789	1.2604	-	-
	$1x10^{-5}$	0.3443	1.002	0.79	79.49
	$5x10^{-5}$	0.2945	1.0394	0.82	82.46
	$1x10^{-4}$	0.1950	1.1142	0.88	88.39
	$5x10^{-4}$	0.1599	1.1406	0.90	90.48
	$1x10^{-3}$	0.1257	1.1664	0.93	92.51
	$5x10^{-3}$	0.1017	1.1845	0.94	93.94
60	0.00	2.9378	2.2056	-	-
	$1x10^{-5}$	0.5250	1.8114	0.82	82.13
	$5x10^{-5}$	0.4381	1.8767	0.85	85.09
	$1x10^{-4}$	0.2861	1.9909	0.90	90.26
	$5x10^{-4}$	0.2311	2.0323	0.92	92.13
	$1x10^{-3}$	0.1761	2.0736	0.94	94.01
	$5x10^{-3}$	0.1403	2.1006	0.95	95.22

Table (3:3): Corrosion rate of carbon steel, surface coverage and percentage inhibition efficiency for carbon steel in 1M HCl in the absence and presence of different concentrations of compound III from weight loss measurements at different temperatures.

Temp. °C	Conc. of inhibitor M	Weight loss (mg)	k mg/cm^2.h	Θ	η_w %
30	0.00	0.5224	0.3922	-	-
	$1x10^{-5}$	0.0880	0.3261	0.83	83.15
	$5x10^{-5}$	0.0681	0.3411	0.87	86.96
	$1x10^{-4}$	0.0600	0.3473	0.89	88.51
	$5x10^{-4}$	0.0491	0.3556	0.91	90.60
	$1x10^{-3}$	0.0454	0.3584	0.91	91.31
	$5x10^{-3}$	0.0353	0.3661	0.93	93.24
40	0.00	0.8816	0.6619	-	-
	$1x10^{-5}$	0.1560	0.5447	0.82	82.30
	$5x10^{-5}$	0.1322	0.5627	0.85	85.00
	$1x10^{-4}$	0.1099	0.5795	0.88	87.53
	$5x10^{-4}$	0.0911	0.5937	0.90	89.67
	$1x10^{-3}$	0.0797	0.6023	0.91	90.96
	$5x10^{-3}$	0.0615	0.6161	0.93	93.02
50	0.00	1.6789	1.2604	-	-
	$1x10^{-5}$	0.2563	1.068	0.85	84.73
	$5x10^{-5}$	0.1971	1.1125	0.88	88.26
	$1x10^{-4}$	0.1593	1.141	0.91	90.51
	$5x10^{-4}$	0.1226	1.1686	0.93	92.70
	$1x10^{-3}$	0.1077	1.1799	0.94	93.59
	$5x10^{-3}$	0.0809	1.2001	0.95	95.18
60	0.00	2.9378	2.2056	-	-
	$1x10^{-5}$	0.3515	1.9417	0.88	88.04
	$5x10^{-5}$	0.2700	2.0029	0.91	90.81
	$1x10^{-4}$	0.2151	2.0442	0.93	92.68
	$5x10^{-4}$	0.1691	2.0788	0.94	94.24
	$1x10^{-3}$	0.1465	2.0959	0.95	95.01
	$5x10^{-3}$	0.1052	2.127	0.96	96.42

3.4 Potentiodynamic polarization technique

The technique of potentiodynamic polarization of metals is frequently used to study the phenomena of metal corrosion and passivation. It yields useful information on the electrode behavior, action of inhibitive and aggressive anions and the effect of the environmental condition. In this technique, an external applied electric current is used and can be varied as will; the experimental can be performed in relatively short time. When a Tafel equation is applicable for both anodic and cathodic polarization, the point of intersection of the two Tafel lines was corresponding to the stationary conditions of corrosion. The function of a substances as inhibitor or stimulator may thus be due to its effect on polarization curves, and consequent displacement of the point of intersection.

The extrapolation of anodic and/or cathodic Tafel lines of charge transfer controlled corrosion reaction gives the corrosion current density, I_{corr} at corrosion potential, E_{corr}. This method is based on the electrochemical theory of corrosion processes developed by Wagner and Traud [139]. Corrosion rates are determined through polarization curves. Polarization curves are produced through the application of current to the metal surface. If the potential of the metal surface is polarized by the current is positive sense it is referred to as being anodically polarized; a negative sense signifies that it is cathodically polarized. The degree of polarization is a measure of how the rates of the anodic and cathodic reactions are hindered by various environmental and surface process factors. The environmental factors (the concentration of metal ions, dissolved oxygen in the solution, etc.) are referred to as concentration polarization. The surface process factors (film formation, adsorption, etc.) are referred to as the activation polarization. The polarization curve is a graph of the variation of potential as a function of current, which allows

the effects of concentration and activation processes on the rate at which anodic or cathodic reactions can give or receive electrons to be determined. This allows for a rate determination for the reactions that are involved in the corrosion process.

The potential, E, is plotted as a function of logarithm of current density (I) show the polarization curves for both anodic and cathodic reactions.

Figs. (3:12-3:14) represent the potentiodynamic polarization plots for carbon steel electrode in 1M HCl in the absence and presence of different concentrations of synthesized compound I, compound II and compound III at scanning rate 2mV/sec.

Inspection of these figures revealed that, there is a transition region at the beginning of the cathodic or anodic polarization known as pre-Tafel region. This region starts from the corrosion potential and extended to the beginning of Tafel region. It is characterized by simultaneous occurrence of cathodic hydrogen evolution reaction and anodic dissolution of the C-steel. The hydrogen evolution leads to cover a fraction (Θ_H) of the electrode surface by the adsorbed hydrogen atoms $(MH)_{ads}$ and the anodic reaction causes a coverage of fraction (Θ_{OH}) of the same electrode by the absorbed OH- groups $(MOH)_{ads}$. These two reactions are in competition and hence give rise to mixed kinetics. Mc Cafferty et al [140] and other [141] considered that, at corrosion potential almost the whole electrode surface is covered by $(MH)_{ads}$ and consequently the coverage fraction (Θ_H) is closed to unity at cathodic potential and decrease when anodic polarization is increased. At the end of transition region there is a metal dissolution, in case of anodic polarization, and the current becomes purely anodic. In case of cathodic polarization the current becomes purely cathodic due to the hydrogen evolution reaction.

The data reveals that, by increasing concentration of the inhibitor compounds cause a decrease in rate of anodic dissolution reaction shifting the anodic current-potential curves in the anodic direction. This may be ascribed to a parallel adsorption of additive compounds over corroding surface.

In the case of the potentiodynamic polarization method, the percentage inhibition efficiency η_p % is defined as the percentage inhibition of the relative decrease in corrosion rate brought about by the percentage of a certain concentration of inhibitor is given by:

$$\eta_p \% = \{(I_{corr} - I_{corr}(inh))/ I_{corr}\} \times 100 \qquad (3:4)$$

where, I_{corr} and $I_{corr(inh)}$ are the corrosion current densities in absence and presence of inhibitors, respectively, determined by extrapolation of cathodic Tafel lines to the corrosion potential.

The degree of surface coverage (Θ) was calculated the following equation:

$$\Theta = \{(I_{corr} - I_{corr\ (inh)})/ I_{corr}\} \qquad (3:5)$$

Tables (3:4-3:6) show the effect of three compounds of cationic gemini surfactants (compound I, compound II and compound III) concentration on some electrochemical parameters e.g. corrosion current density (I_{cror}), corrosion potential (E_{corr}), anodic and cathodic Tafel slopes (β_a and β_c), the degree of surface coverage (Θ) and the percentage of inhibition efficiency (η_p %) during the corrosion of C-steel electrode in 1M HCl solutions.

Inspection of these tables:

1. The corrosion potential (E_{corr}) values was slightly shifted to negative values by increasing the concentration of the inhibitors.

2. decrease the values of I_{corr}, indicating the inhibiting effect of these compounds toward the dissolution of C-steel electrode in 1M HCl solution.
3. The Tafel polarization curves indicate that the inhibitors act as mixed type of inhibitor because in the presence of inhibitor, the cathodic and anodic curves are shifted towards more negative and positive directions, respectively. Also, the values of βa and βc are changed slightly by increased the concentration of inhibitors [142].
4. The percentage inhibition efficiency value increasing with increase in concentration of inhibitor, which indicates higher surface coverage of the metal. The corrosion resistance is related to the formation of adsorbed film on the steel surface, which was further supported by SEM images of the electrode surface [143].
5. At one and the same concentration of the inhibitors, the order of inhibition efficiency of cationic gemini surfactants decreases in the following order:

compound III >compound II > compound I.

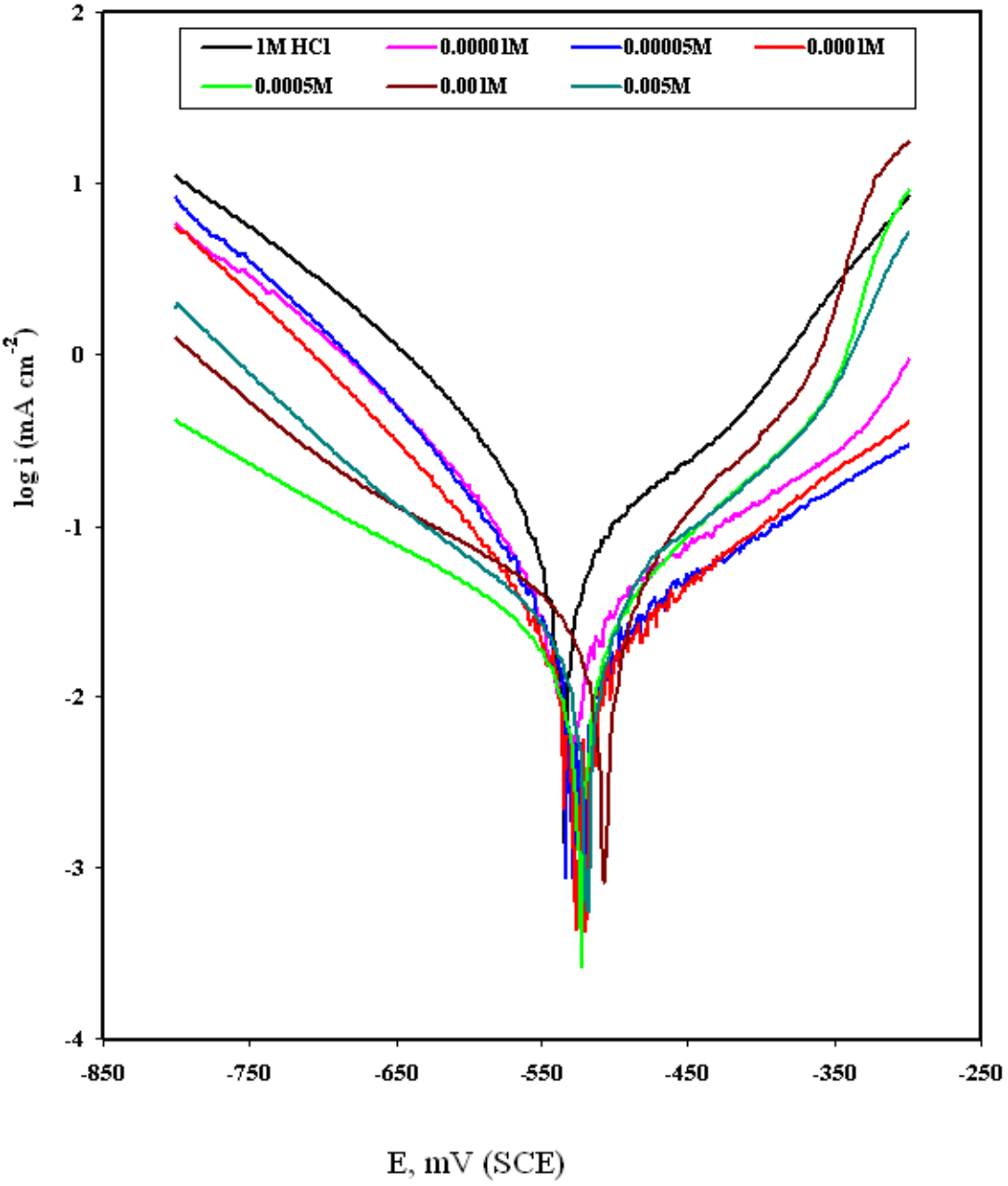

Fig. (3:12): Potentiodynamic polarization curves for the carbon steel in 1M HCl in the absence and presence of different concentrations of compound I at scanning rate 2 mV s^{-1}.

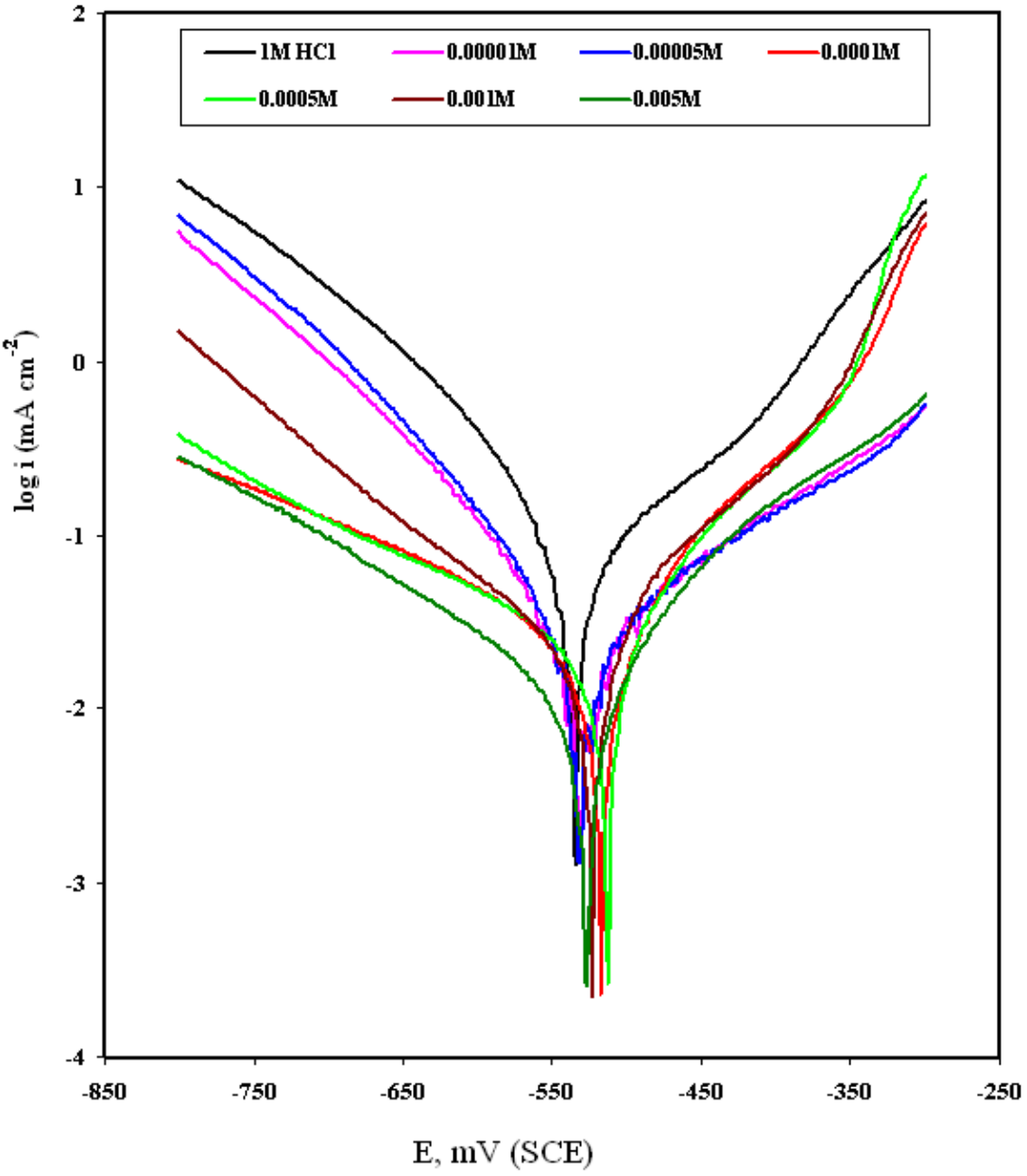

Fig. (3:13): Potentiodynamic polarization curves for the carbon steel in 1M HCl in the absence and presence of different concentrations of compound II at scanning rate 2 mV s^{-1}.

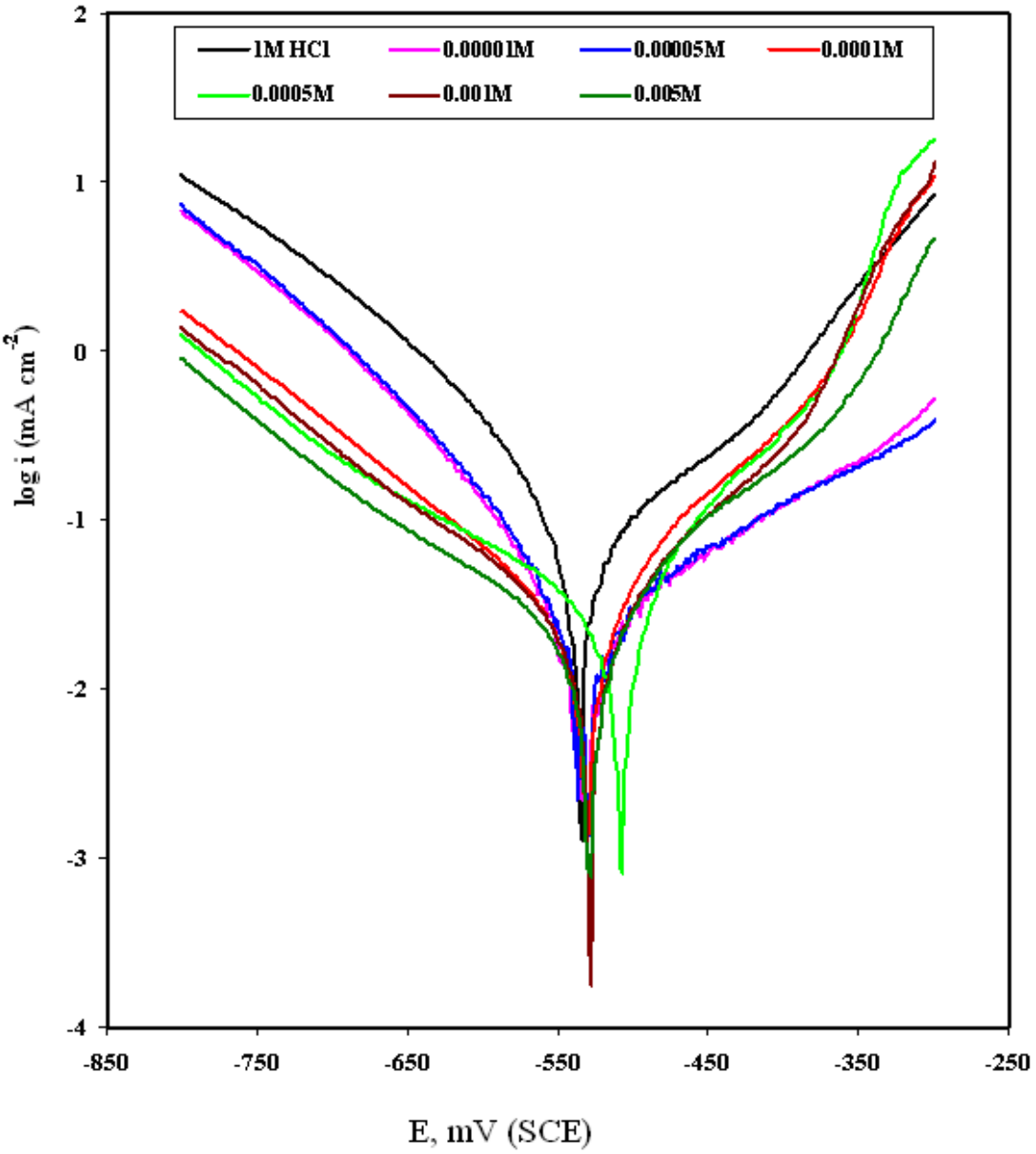

Fig. (3:14): Potentiodynamic polarization curves for the carbon steel in 1M HCl in the absence and presence of different concentrations of compound III at scanning rate 2mV s^{-1}.

Table (3:4): Potentiodynamic polarization parameters for corrosion of carbon steel in 1M HCl in absence and presence of different concentrations of compound I at 30°C at scanning rate $2mVs^{-1}$.

Conc. of inhibitor M	E_{corr} mV (SCE)	I_{corr} mA cm^{-2}	β_a mV dec^{-1}	β_c mV dec^{-1}	Θ	η_p %
0.00	-534	0.2271	124	-140	-	-
$1x10^{-5}$	-533	0.0666	310	-131	0.67	67.67
$5x10^{-5}$	-527	0.0405	280	-112	0.80	80.34
$1x10^{-4}$	-527	0.0259	193	-113	0.87	87.43
$5x10^{-4}$	-526	0.0195	119	-212	0.90	90.53
$1x10^{-3}$	-510	0.0169	78	-160	0.91	91.84
$5x10^{-3}$	-521	0.0150	107	-137	0.92	92.72

Table (3:5): Potentiodynamic polarization parameters for corrosion of carbon steel in 1M HCl in absence and presence of different concentrations of compound II at 30^{o}C at scanning rate 2 mV s^{-1}.

Conc. of inhibitor M	E_{corr} mV (SCE)	I_{corr} mA cm^{-2}	β_a mV dec^{-1}	β_c mV dec^{-1}	Θ	η_p %
0.00	-534	0.2271	124	-140	-	-
1x10^{-5}	-532	0.0478	241	-128	0.76	76.80
5x10^{-5}	-532	0.0371	225	-109	0.81	81.99
1x10^{-4}	-520	0.0277	119	-281	0.88	88.98
5x10^{-4}	-515	0.0192	104	-233	0.90	90.68
1x10^{-3}	-525	0.0153	101	-142	0.92	92.57
5x10^{-3}	-528	0.133	111	-201	0.93	93.54

Table (3:6): Potentiodynamic polarization parameters for corrosion of carbon steel in 1M HCl in absence and presence of different concentrations of compound III at 30^{o}C at scanning rate 2 mV s^{-1}.

Conc. of inhibitor M	E_{corr} mV (SCE)	I_{corr} mA cm^{-2}	β_a mV dec^{-1}	β_c mV dec^{-1}	Θ	η_p %
0.00	-534	0.2271	124	-140	-	-
$1x10^{-5}$	-534	0.0302	210	-101	0.85	85.34
$5x10^{-5}$	-532	0.0263	193	-92	0.87	87.23
$1x10^{-4}$	-532	0.0218	107	-139	0.89	89.42
$5x10^{-4}$	-510	0.0169	77	-165	0.91	91.80
$1x10^{-3}$	-529	0.0145	100	-135	0.92	92.96
$5x10^{-3}$	-530	0.0113	103	-143	0.94	94.51

3.5 Electrochemical impedance spectroscopy (EIS)

EIS or ac impedance methods have seen tremendous increase in popularity in recent years. Initially applied to the determination of the double-layer capacitance and in ac polarography, they are now applied to the characterization of electrode processes and complex interfaces. EIS studies the system response to the application of a periodic small amplitude ac signal. These measurements are carried out at different ac frequencies and, thus, the name impedance spectroscopy was later adopted. Analysis of the system response contains information about the interface, its structure and reactions taking place there [144].

The corrosion behavior of C-steel in 1M HCl solution in the absence and presence of the studied cationic gemini surfactants (compound I, compound II and compound III) was investigated by EIS method at 30°C.

The impedance spectra of different Nyquist plots were analyzed by fitting the experimental data to a simple equivalent circuit model which shown in Fig. (3:15), which includes the solution resistant R_s and the double layer capacitance C_{dl} which is placed in parallel to the charge transfer resistance R_{ct}.

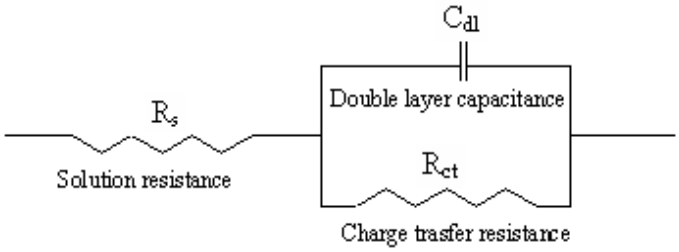

Fig. (3:15): Electrical equivalent circuit used for modeling the interface C-steel/1M HCl solution in the absence and presence of the prepared cationic gemini surfactants.

Figs. (3:16-3:18) show the Nyquist plots for carbon steel in 1M HCl solution in the absence and presence of different concentrations of inhibitors at 30^{o}C. The Nyquist plots were regarded as one part of a semicircle. The impedance diagram shows the same trend (one capacitive loop), however, the diameter of this capacitive loop increases with increasing concentration.

It is clear that the shapes of the impedance plots for inhibited electrodes are not substantially different from those of uninhibited electrodes. The presence of the inhibitor increases the impedance but does not change other aspects of the behavior. These results support the results of polarization measurements that the inhibitor does not alter the electrochemical reactions responsible for corrosion. It inhibits corrosion primarily through its adsorption on the metal surface [136].

The main parameters deduced from the analysis of Nyquist diagram are:

i. The resistance of charge transfer R_{ct}.

ii. The capacity of double layer C_{dl}.

The charge transfer resistance values (R_{ct}) are calculated from the difference in impedance at lower and higher frequencies, as suggested by Haruyama and Tsuru [145]. To obtain the double-layer capacitance (C_{dl}), the frequency at which the imaginary component of the impedance at maximum f($-Z''_{img}$) is found and C_{dl} values are calculated from the following equation [144]:

$$f(-Z''_{img}) = 1/(2\pi C_{dl} R_{ct}) \qquad (3:6)$$

The impedance quantitative results can be seen in Tables (3:7-3:9). It is clear that, the corrosion of steel is obviously inhibited in the presence of the inhibitors. It is apparent that, the impedance response for carbon steel in HCl changes significantly with increasing inhibitor concentration.

In the case of the electrochemical impedance spectroscopy, the inhibition efficiency is calculated using charge transfer resistance as follow [146]:

$$\eta_Z\ \% = \{(R_{ct(inh)}-R_{ct}) / R_{ct(inh)}\} \times 100 \qquad (3:7)$$

where, R_{ct} and R_{ct}(inh) are the charge transfer resistance values in the absence and presence of inhibitors for C steel in 1M HCl, respectively.

As the inhibitor concentration increased, the R_{ct} values increased, but the C_{dl} values tended to decrease. The decrease in C_{dl} value is due to the adsorption of inhibitor on the metal surface [147]. The inhibition efficiency increases with increasing inhibitor concentration. This fact suggests that the inhibitor molecules may first be adsorbed on the steel surface and cover some sites of the electrode surface. These layers protect steel surface. The order of percentage inhibition efficiency decreases in the following order:

compound III > compound II > compound I.

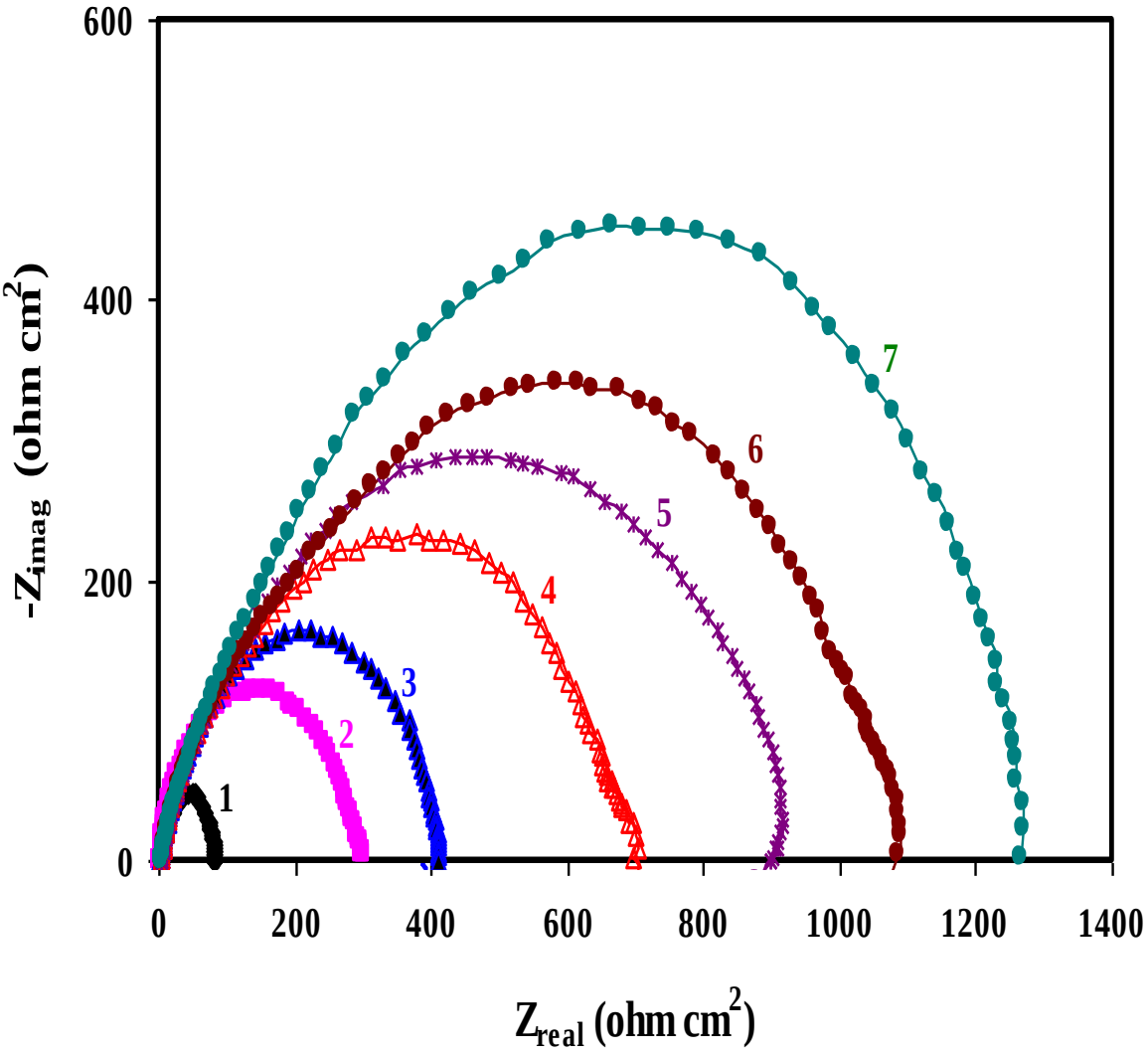

Fig. (3:16): Nyquist plots for the carbon steel in 1M HCl in the absence and presence of different concentrations of compound I.

where, 1) 0.00M 2) $1x10^{-5}$M 3) $5x10^{-5}$M 4) $1x10^{-4}$M 5) $5x10^{-4}$M 6) $1x10^{-3}$M 7) $5x10^{-3}$M of compound I.

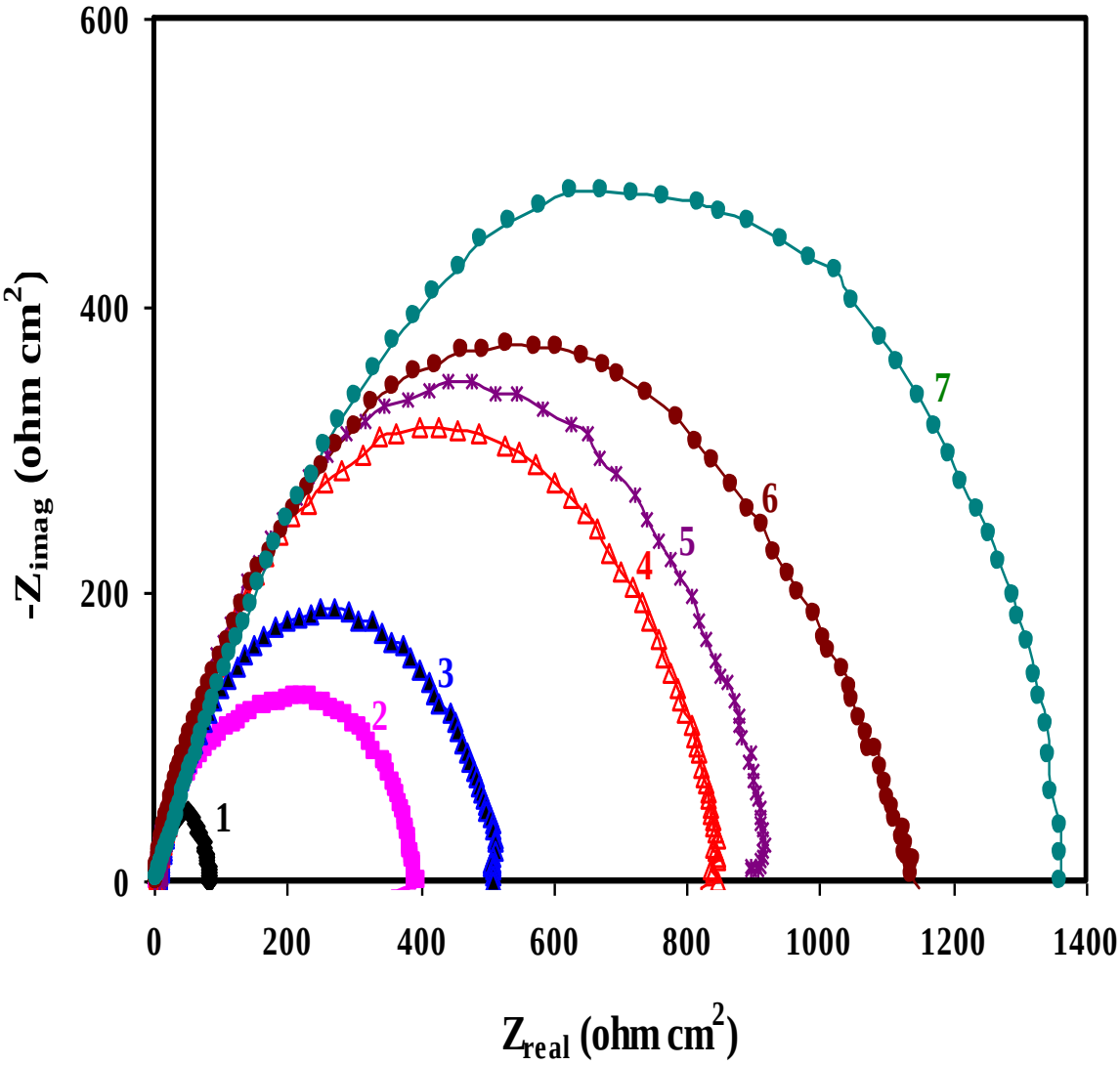

Fig. (3:17): Nyquist plots for the carbon steel in 1M HCl in the absence and presence of different concentrations of compound II.

where, 1) 0.00M 2) $1x10^{-5}$M 3) $5x10^{-5}$M 4) $1x10^{-4}$M 5) $5x10^{-4}$M 6) $1x10^{-3}$M 7) $5x10^{-3}$M of compound II.

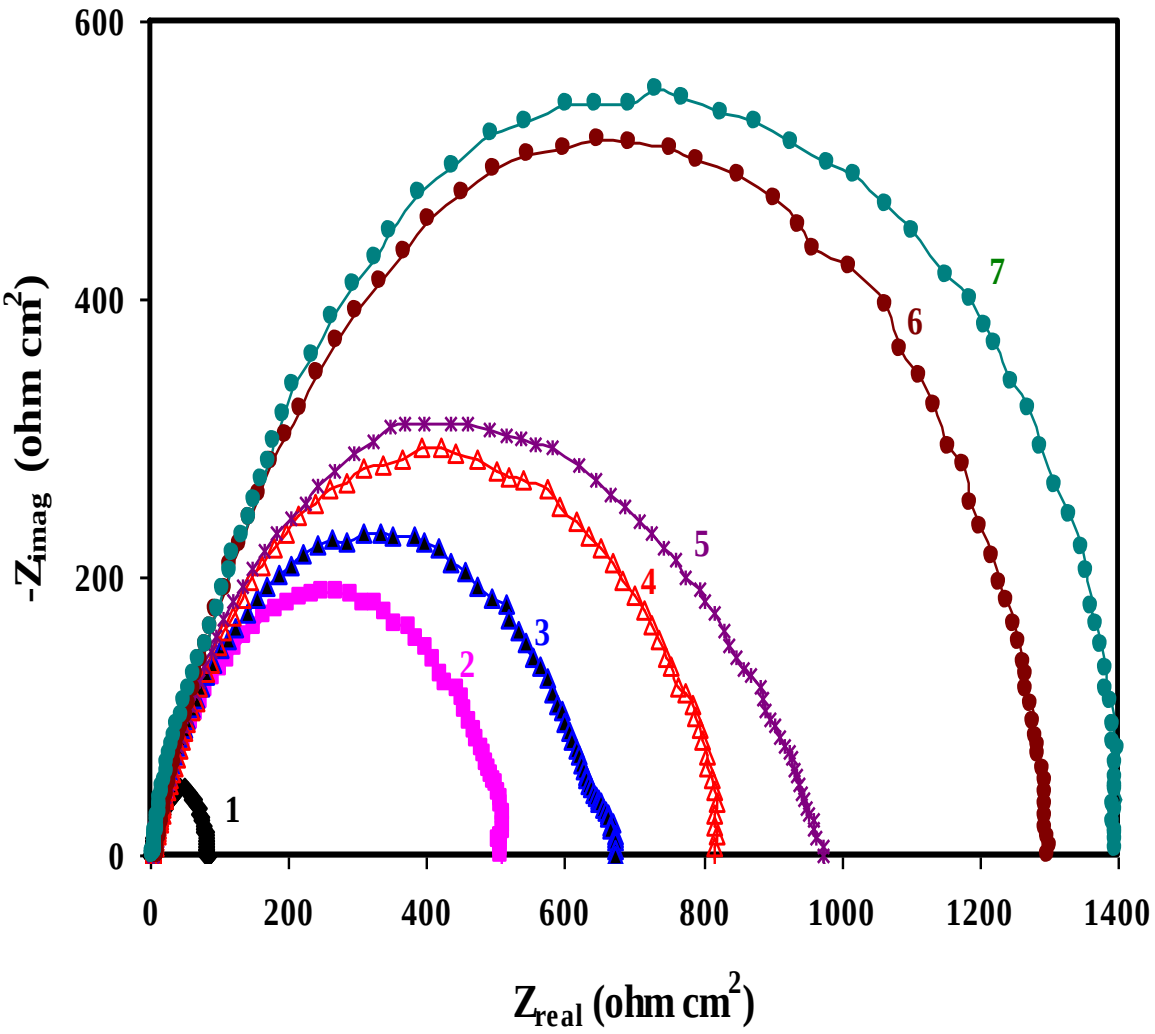

Fig. (3:18): Nyquist plots for the carbon steel in 1M HCl in the absence and presence of different concentrations of compound III.

where, 1) 0.00M 2) $1x10^{-5}$M 3) $5x10^{-5}$M 4) $1x10^{-4}$M 5) $5x10^{-4}$M 6) $1x10^{-3}$M 7) $5x10^{-3}$M of compound III.

Table (3:7): EIS parameters for corrosion of carbon steel in 1M HCl in the absence and presence of different concentrations of compound I at 30°C.

Conc. of inhibitor M	R_s ohm cm^2	R_{ct} ohm cm^2	C_{dl} $\mu F\ cm^{-2}$	Θ	η_Z %
0.00	1.12	87.0	112.2	-	-
$1x10^{-5}$	1.19	294.6	35.33	0.70	70.47
$5x10^{-5}$	2.95	412.1	26.40	0.78	78.89
$1x10^{-4}$	1.98	696.0	25.60	0.87	87.50
$5x10^{-4}$	2.78	902.2	24.33	0.90	90.36
$1x10^{-3}$	2.98	1050.0	14.88	0.91	91.71
$5x10^{-3}$	3.17	1298.0	8.982	0.93	93.30

Table (3:8): EIS parameters for corrosion of carbon steel in 1M HCl in the absence and presence of different concentrations of compound II at 30°C.

Conc. of inhibitor M	R_s ohm cm^2	R_{ct} ohm cm^2	C_{dl} µF cm^{-2}	Θ	η_Z %
0.00	1.12	87.0	112.2	-	-
$1x10^{-5}$	2.43	390	33.67	0.77	77.69
$5x10^{-5}$	2.61	490.6	24.38	0.82	82.27
$1x10^{-4}$	2.91	841.3	20.39	0.89	89.66
$5x10^{-4}$	2.96	913.7	18.56	0.90	90.48
$1x10^{-3}$	2.35	1103	17.18	0.92	92.11
$5x10^{-3}$	2.46	1339	11.88	0.93	93.50

Table (3:9): EIS parameters for corrosion of carbon steel in 1M HCl in the absence and presence of different concentrations of compound III at 30^{o}C

Conc. of inhibitor M	R_s ohm cm^2	R_{ct} ohm cm^2	C_{dl} µF cm^{-2}	Θ	η_Z %
0.00	1.12	87.0	112.2	-	-
1x10^{-5}	2.61	490.0	27.92	0.82	82.24
5x10^{-5}	2.47	664.8	26.17	0.86	86.91
1x10^{-4}	2.56	797.8	23.93	0.89	89.10
5x10^{-4}	1.34	960.6	18.16	0.90	90.94
1x10^{-3}	2.54	1282	12.41	0.93	93.21
5x10^{-3}	2.34	1397	8.982	0.94	93.77

3.6 Kinetic parameters

3.6.1 Activation energy

The apparent activation energy, E_a, for the corrosion of C-steel sample in 1M HCl solution in the absence and presence of different concentrations of cationic gemini surfactants, at 30, 40, 50, and 60°C were calculated from Arrhenius equation.

$$k = A\, e^{(-Ea/RT)} \qquad (3.8)$$

and the logarithmic form:

$$\ln k = \ln A - E_a /RT \qquad (3:9)$$

where, k is the corrosion rate, A is the Arrhenuis constant, R is the gas constant and T is the absolute temperature.

Arrhenius plots of ln k vs. 1/T in the absence and presence of different concentrations of compounds (compound I, compound II and compound III) where shown graphically in Figs. (3:19-3:21) give straight lines with slope of ($-E_a/R$). Activation energies were calculated and given in Table (3:10-3:12).

Inspection of Tables (3:10-3:12) the values of activation energy decrease in the presence of inhibitors. The lower value of the activation energy (E_a) in presence of inhibitors is attributed to adsorption of these compounds on the steel surface.

From these results, it is clear that the presence of tested cationic gemini surfactants are decreased the activation values and decreased the corrosion rate of C-steel [143]. Also, activation energy values are decreased by increasing the concentration of inhibitors. These results are indicating that, these tested compounds acted as inhibitors through strong adsorption on C-steel surface by making a barrier to mass and charge transfer. Generally the nature and the concentration of electrolyte affect greatly the activation energy for the corrosion process.

The change in enthalpy and entropy of activation values (ΔH*, ΔS*) were calculated from the transition state theory [148].

$$k = RT/Nh \exp(\Delta S^*/R) \exp(-\Delta H^*/RT) \quad (3:10)$$

where, h is the Plank constant, N is the Avogadros number, and R is the ideal gas constant.

A plot of log (k/T) versus 1/T, gave straight lines as shown in Fig. (3:22) for carbon steel dissolution in 1M HCl in the absence and presence of different concentrations of inhibitors. Straight lines are obtained with a slope of ΔH*/R and an intercept of log (R/Nh) + ΔS*/R. The values of ΔH* and ΔS* werecalculated and listed in Table (3:13). Inspection of these data reveals that the activation parameters (ΔH* and ΔS*) of the dissolution reaction carbon steel in 1M HCl in the presence of the inhibitors are less than that of in the absence of inhibitors. The positive signs of the change in enthalpies (ΔH*) reflect the endothermic nature of the steel dissolution process and means that the dissolution of steel is difficult [149]. The change in entropy of activation in the presence and absence of the inhibitors are negative. This implies that the activated complex the rate-determining step represents association rather than dissociation, indicating that a decrease in disorder takes place, going from reactant to activated complex [150].

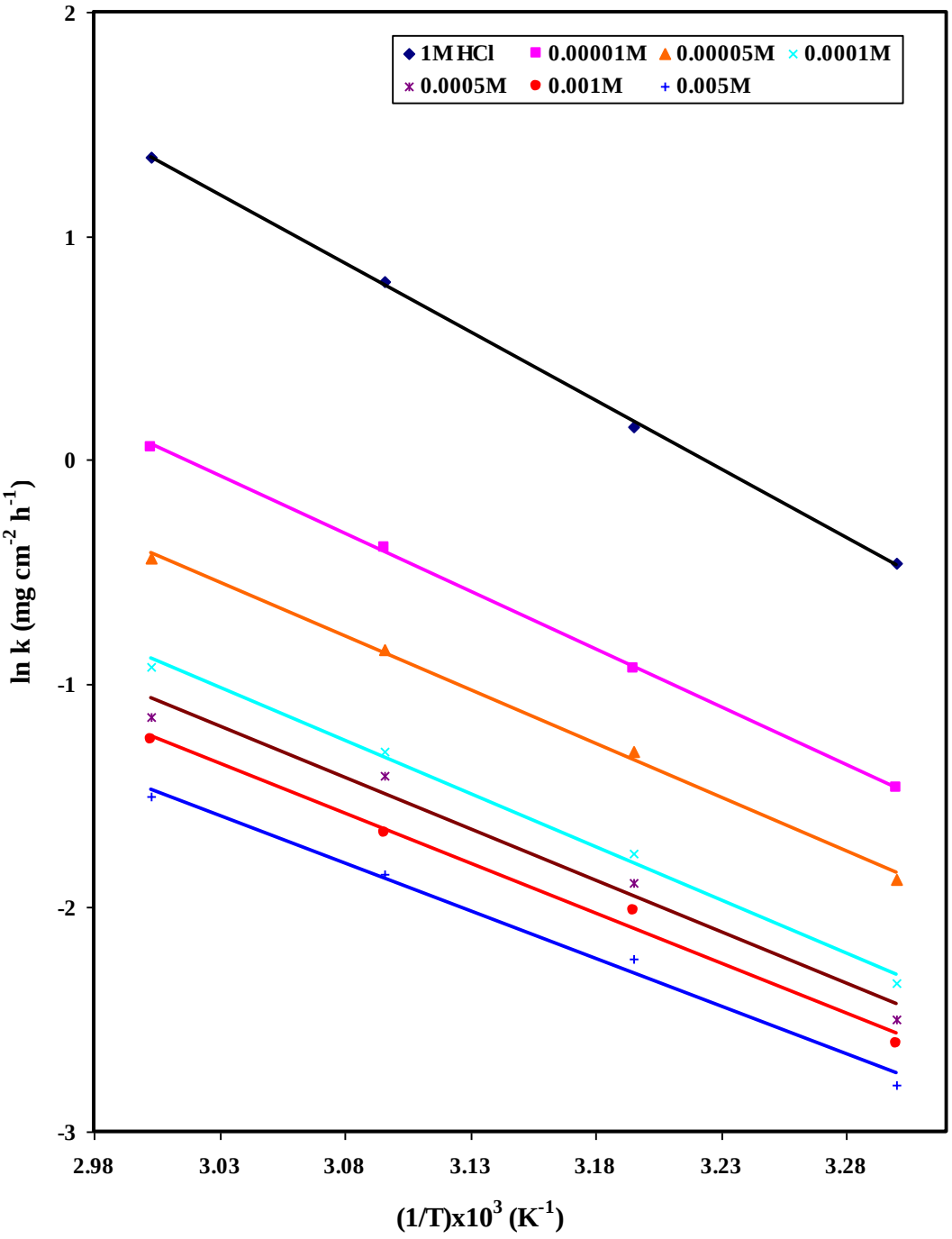

Fig. (3:19): Arrhenius plots (ln k vs. 1/T curves) for carbon steel dissolution in absence and presence of different concentrations of compound I in 1M HCl solution.

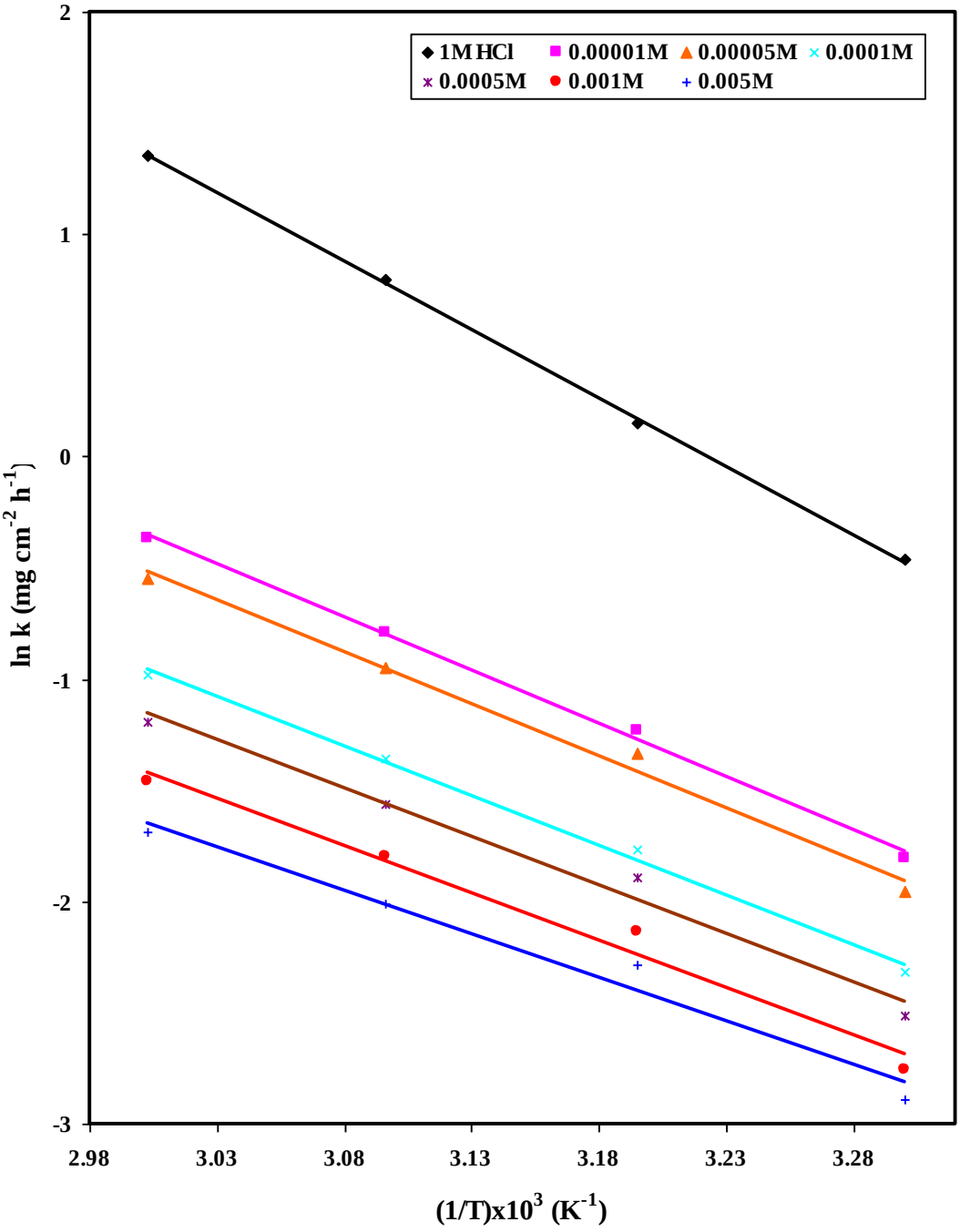

Fig. (3:20): Arrhenius plots (ln k vs. 1/T curves) for carbon steel dissolution in absence and presence of different concentrations of compound II in 1M HCl solution.

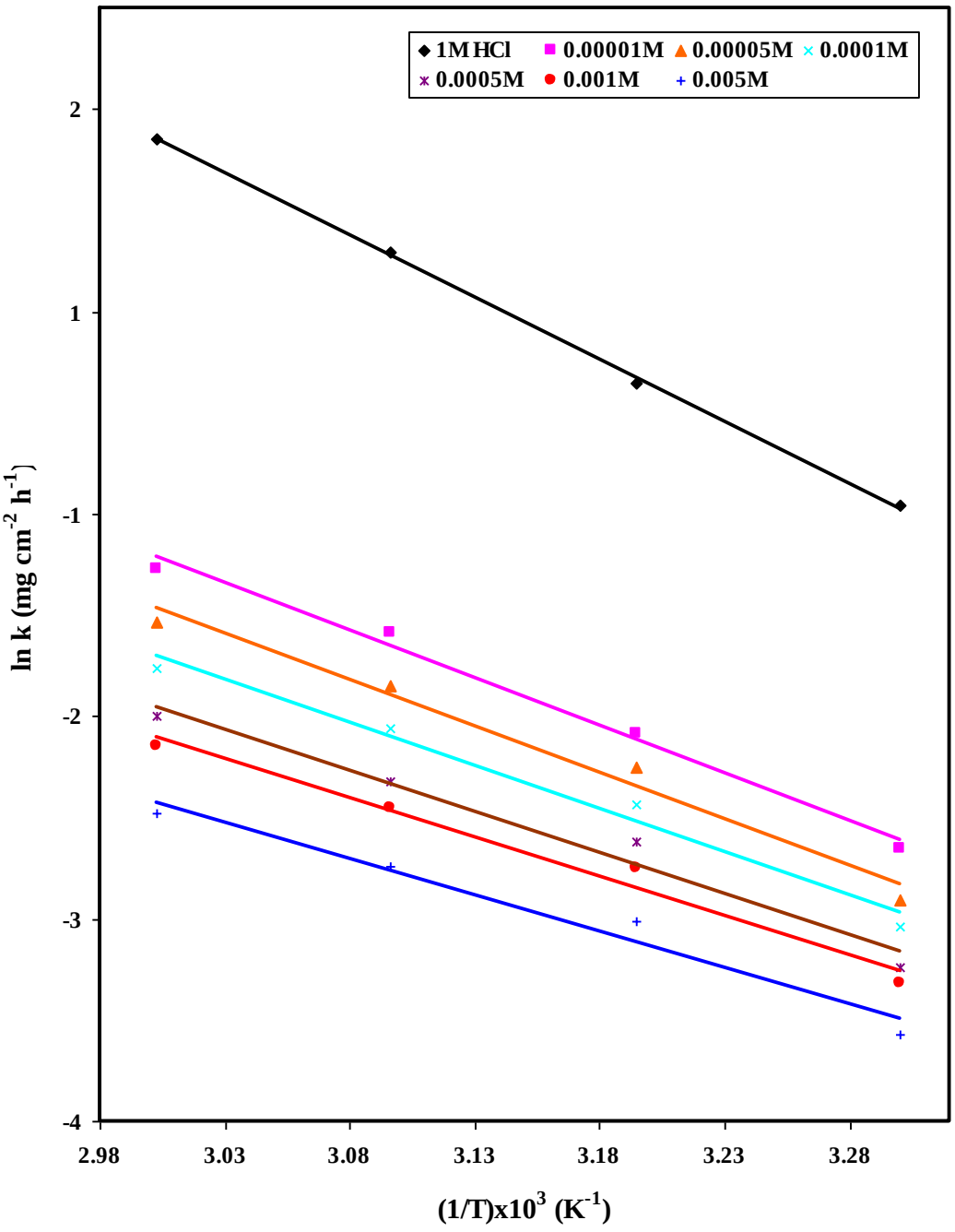

Fig. (3:21): Arrhenius plots (ln k vs. 1/T curves) for carbon steel dissolution in absence and presence of different concentrations of compound III in 1M HCl solution.

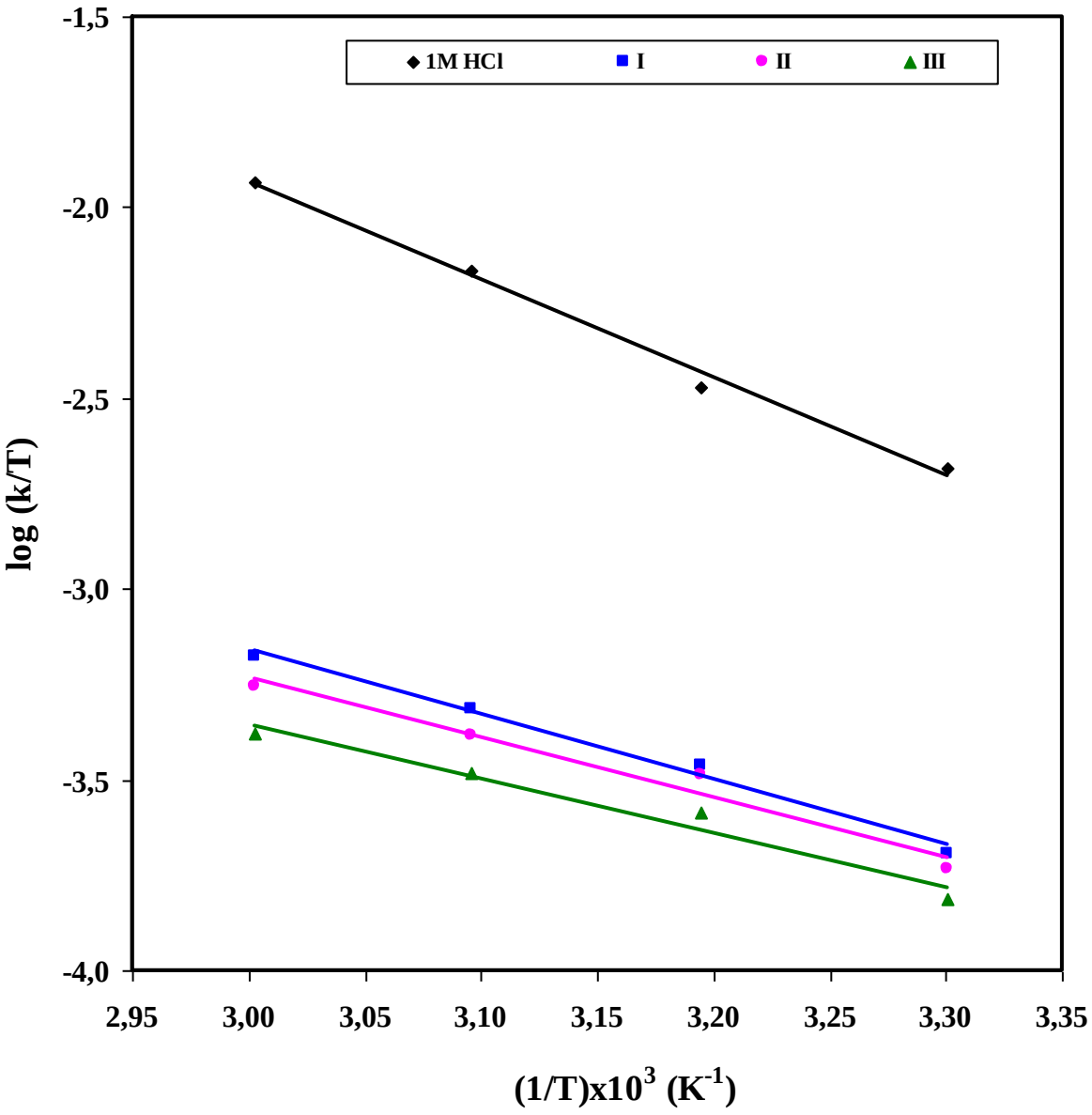

Fig. (3:22): Relationship between log K/T and the reciprocal of the absolute temperature of carbon steel in 1M HCl containing $5x10^{-3}$ M of cationic gemini surfactants.

Table (3:10): Values of activation energy (E_a) for carbon steel in the absence and presence of different concentrations of compound I in 1M HCl at different temperatures.

Conc. of inhibitor M	**E_a kJ mol^{-1}**
0.00	**54.05**
1x10^{-5}	**42.79**
5x10^{-5}	**40.00**
1x10^{-4}	**39.41**
5x10^{-4}	**38.18**
1x10^{-3}	**37.03**
5x10^{-3}	**35.47**

Table (3:11): Values of activation energy (E_a) for carbon steel in the absence and presence of different concentrations of compound II in 1M HCl at different temperatures.

Conc. of inhibitor M	**E_a kJ mol^{-1}**
0.00	**54.05**
1x10^{-5}	**39.78**
5x10^{-5}	**38.77**
1x10^{-4}	**37.24**
5x10^{-4}	**36.15**
1x10^{-3}	**35.47**
5x10^{-3}	**33.03**

Table (3:12) Values of activation energy (E_a) for carbon steel in the absence and presence of different concentrations of compound III in 1M HCl at different temperatures.

Conc. of inhibitor M	**E_a kJ mol^{-1}**
0.00	**54.05**
1x10^{-5}	**39.13**
5x10^{-5}	**38.18**
1x10^{-4}	**35.39**
5x10^{-4}	**33.75**
1x10^{-3}	**32.13**
5x10^{-3}	**29.92**

Table (3:13): Activation thermodynamic parameters for carbon steel in the absence and presence of 5x10^{-3}M of cationic gemini surfactants in 1M HCl at different temperatures.

Inhibitors	**ΔH* KJmol^{-1}**	**ΔS* KJmol^{-1}K^{-1}**
Absence	**49,10**	**-29,728**
compound I	**32,88**	**-101,86**
compound II	**29,95**	**-112,14**
compound III	**27,28**	**-122,47**

3.6.2 Adsorption isotherm

The type of adsorption isotherm and the effect of temperature on the corrosion rate was studied. It is generally accepted that the cationic gemini surfactants, compounds inhibit the corrosion process by adsorbing at the metal/solution interface. However, the modes of adsorption are dependent on:

i. Chemical structure of molecule.
ii. Chemical composition of solution.
iii. Nature of the metal surface.
iv. Electrochemical potential at the interface, one or a combination of more of three principle types of adsorption: π bond, electrostatic and chemisorption [151].

In addition, it is believed that the formation of a solid organic molecule complex with the metal atom has received considerable attention [152].

When designing inhibitor, all of theories are in common agreement that an adsorption phenomenon involve either:-

i. Proton acceptor (cathodic site adsorbers), material in this group accepts the hydrogen ions or proton and migrates to the cathode.]
ii. Electron acceptor (anodic site adsorbers), inhibitor functions due to their ability to accept electrons.
iii. Adsorb at anodic and cathodic sites.

It has been generally accepted that group contributions vary considerably from molecule to molecule. Utilization of these concepts permits the systematic construction of an increasing efficiency of molecule.

The adsorption behavior of the additives on the metal surface can be interpreted by finding a suitable isotherm which describes the variation of experimentally obtained values of the amounts of adsorbed substances

by unit area of metal surface with its concentration in the bulk of solution at constant temperature.

The additive cationic gemini surfactants inhibit the corrosion process by adsorption on metal surface. Theoretically, the adsorption process can be regarded as a single substitution process in which an inhibitor molecule, I, in the aqueous phase substitutes an "x" number of water molecules adsorbed on the metal surface, equation (1:6). The adsorption depends on the structure of inhibitor, the type of the metal and the nature of its surface, the nature of the corrosion medium, the pH value, and the interface. Also, the adsorption provides information about the interaction among the adsorbed molecules themselves as well as their interaction with the metal surface. Actually an adsorbed molecule may make the surface more difficult or less difficult for another molecule to become attached to a neighboring site and multilayer adsorption may take place. Finally, various surface sites could have varying degree of activation. For these reasons a number of mathematical adsorption isotherm expressions have been developed, as has been mentioned in chapter (1). A number of mathematical relationships for adsorption isotherms have been suggested to fit the experimental data of the present work.

The equation that fits our results is that due to Langmuir isotherm and is given by the general equation:

$$C/\Theta = 1/ K_{ads} + C \qquad (3:11)$$

where, K and C are the equilibrium constant of adsorption process and additive concentration, respectively.

The degrees of surface coverage (θ) for different concentrations of inhibitors in 1M HCl solution have been calculated from weight loss measurements by using equation (3:1).

In these cases, the plots of C/θ versus C yield a straight line with intercept of (1/ K_{ads}) with slope closed to 1 Figs. (3:23 -3:25). This indicates that, the adsorption of cationic gemini surfactants on the carbon steel surface in 1M HCl solution follows Langmuir's adsorption isotherm and consequently, these is no interaction between the molecules adsorbed at the surface. The free energy of adsorption (ΔG_{ads}) at different temperatures was calculated from the following equation [153]:

$$-\Delta G_{ads} = RT \ln (55.5\ K_{ads}) \qquad (3:12)$$

where, C is the inhibitor concentration, θ is the fraction of the surface covered, K_{ads} is the equilibrium constant of the inhibitor adsorption process, the value 55.5 is the molar concentration of water in solution in mol dm^{-3}, R is the gas constant, T is the absolute temperature and ΔG_{ads} is the standard free energy of adsorption.

The heat of adsorption (Q_{ads}), which is obtained from the slopes of the straight lines when K_{ads} plot versus 1/T, is equal to $-Q_{ads}/R$. Since the pressure is a constant, Q_{ads} is equal to enthalpy of adsorption (ΔH_{ads}) with good approximation. Then ΔH_{ads} value is equal to 3.64, 3.44 and 5.15 kJ. mol^{-1} for compound I, compound II and compound III, respectively. The positive values of ΔH_{ads} indicated that the adsorption of investigated inhibitors on the carbon steel surface in 1M HCl is endothermic process.

The calculated values of the adsorption free energy, ΔG_{ads}, adsorption entropies, ΔS_{ads}, and adsorption enthalpies, ΔH_{ads}, are given in Tables (3:22-3:24). Generally, values of ΔG_{ads} around −20 kJ mol^{-1} or lower are consistent with the electrostatic interaction between the charged molecules and the charged metal (physisorption). While those more negative than −40 kJ mol^{-1} involve charge sharing or transfer from the inhibitor molecules to the metal surface to form a coordinate type of bond (chemisorption) [154,155]. The calculated ΔG_{ads} values indicated that the adsorption mechanism of the prepared cationic gemini surfactants on

carbon steel in 1M HCl solution is a mixed physical and chemical adsorption. The large values of ΔG_{ads} and its negative sign are usually characteristic of strong interaction and a highly efficient adsorption [156].

Entropy of inhibitor adsorption (ΔS_{ads}) can be calculated using the following equation:

$$\Delta G_{ads} = \Delta H_{ads} - T\,\Delta S_{ads} \qquad (3:13)$$

It is clear that from Tables (3:14-3:16), ΔS_{ads} values in the presence of the prepared cationic gemini surfactants has a positive sign meaning that an increase in ordering takes place in going from reactants to the M_{ads} reaction complex.

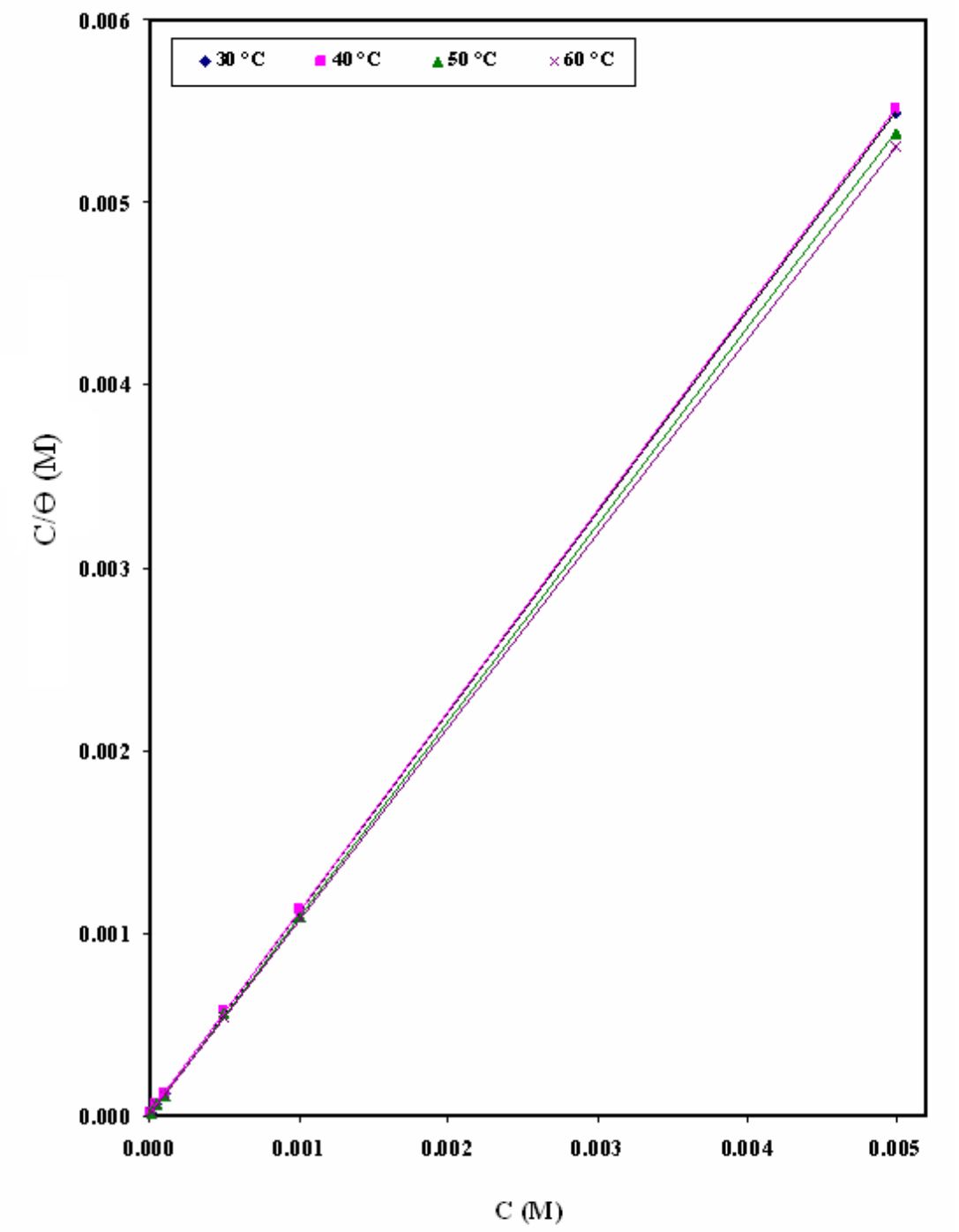

Fig. (3:23): Langmuir isotherm adsorption model on the carbon steel surface of compound I in 1M HCl at different temperatures.

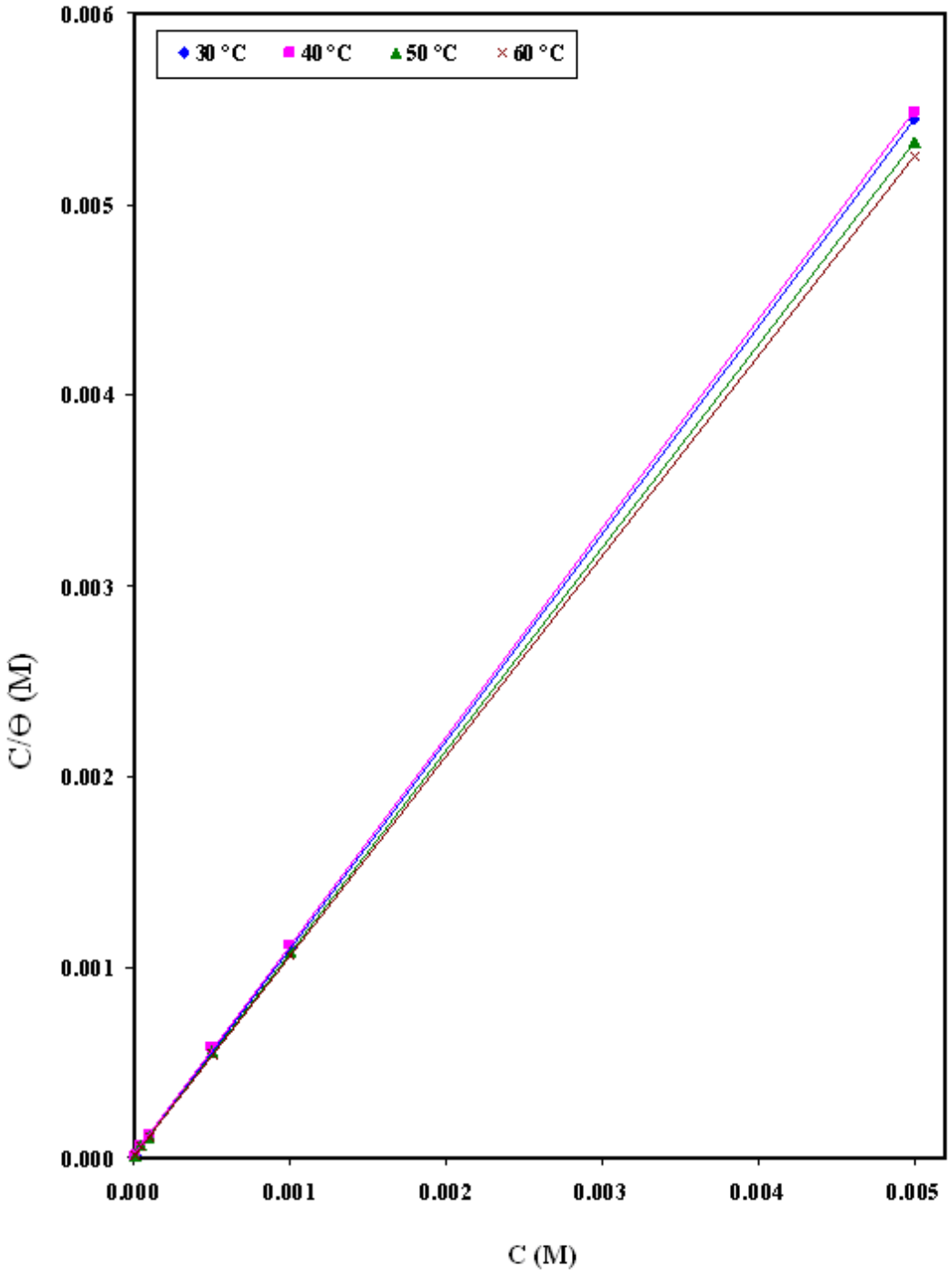

Fig. (3:24): Langmuir isotherm adsorption model on the carbon steel surface of compound II in 1M HCl at different temperatures.

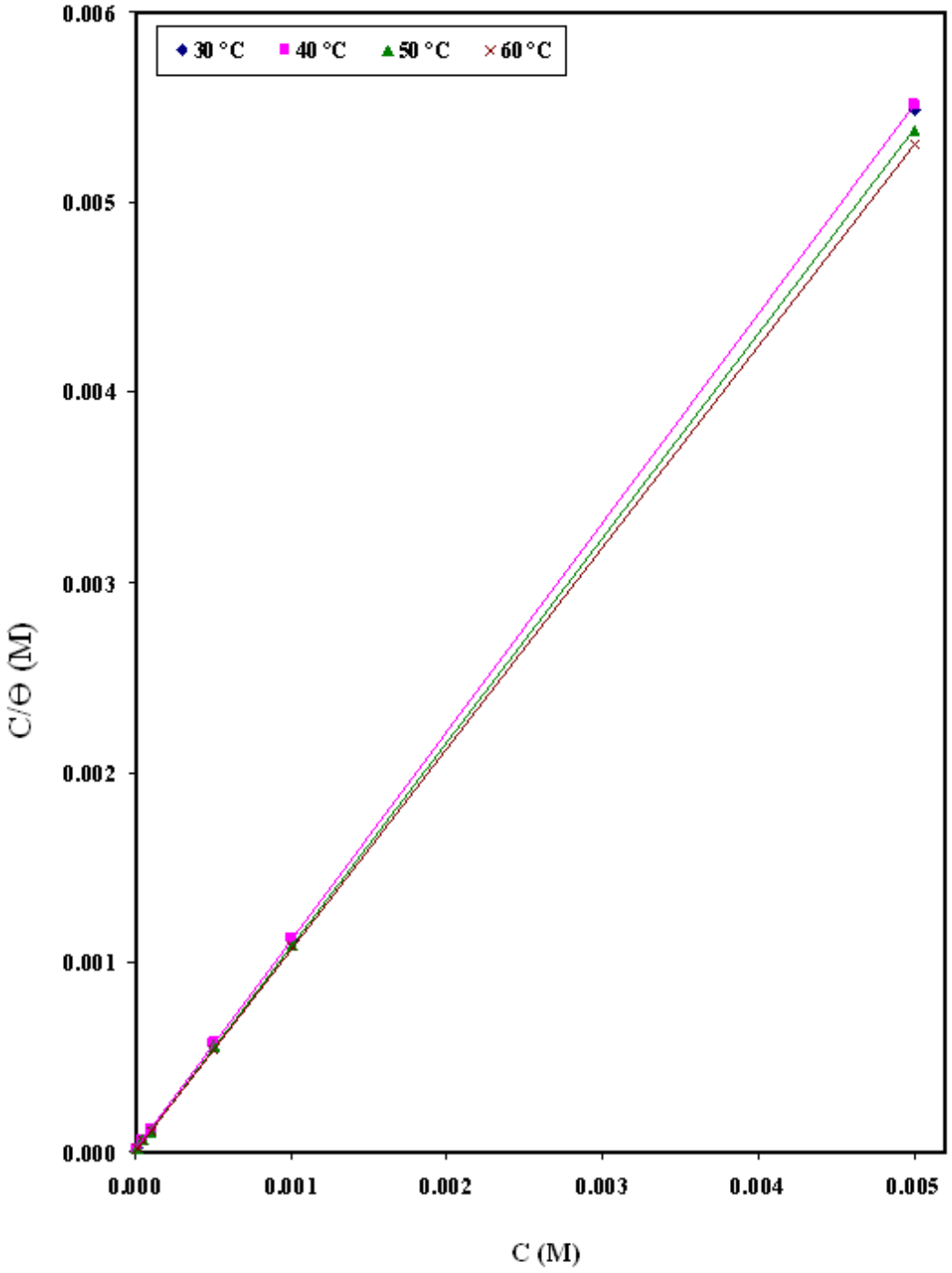

Fig. (3:25): Langmuir isotherm adsorption model on the carbon steel surface of compound III in 1M HCl at different temperatures.

Table (3:14): Thermodynamic parameters of adsorption on carbon steel surface in 1M HCl containing different concentrations of compound I at different temperatures.

Temp. ^{o}C	**K_{ads} x10^{-4} M^{-1}**	**ΔG_{ads} kJ mol^{-1}**	**ΔH_{ads} kJ mol^{-1}**	**ΔS_{ads} J mol^{-1} K^{-1}**
30	**8.13**	**-37.33**	**3.64**	**139.81**
40	**6.94**	**-39.46**		**137.70**
50	**8.33**	**-42.49**		**138.52**
60	**10.31**	**-45.67**		**139.67**

Table (3:15): Thermodynamic parameters of adsorption on carbon steel surface in 1M HCl containing different concentrations of compound II at different temperatures.

Temp. ^{o}C	**K_{ads} x10^{-4} M^{-1}**	**ΔG_{ads} kJ mol^{-1}**	**ΔH_{ads} kJ mol^{-1}**	**ΔS_{ads} J mol^{-1} K^{-1}**
30	**8.85**	**-37.53**	**3.44**	**139.85**
40	**7.81**	**-39.77**		**138.06**
50	**9.43**	**-42.83**		**138.97**
60	**10.99**	**-45.85**		**139.65**

Table (3:16): Thermodynamic parameters of adsorption on carbon steel surface in 1M HCl containing different concentrations of compound III at different temperatures.

Temp. ^{o}C	**K_{ads} x10^{-4} M^{-1}**	**ΔG_{ads} kJ mol^{-1}**	**ΔH_{ads} kJ mol^{-1}**	**ΔS_{ads} J mol^{-1} K^{-1}**
30	**10.42**	**-37.93**	**5.15**	**147.02**
40	**8.85**	**-40.09**		**144.54**
50	**11.90**	**-43.48**		**146.02**
60	**14.29**	**-46.62**		**146.66**

3.7 Scanning electron microscope (SEM)

The scanning electron microscope images were recorded Fig. (3:26a–d) to establish the interaction of organic molecules with the metal surface. The SEM images show the features of carbon steel surface after immersed for 24 h in 1M HCl in absence and presence of $5x10^{-3}$ M each of compound I, compound II and compound III, respectively. The images of SEM revealed that the specimens immersed in the inhibitor solutions are in better conditions having smooth surface while the metal surface immersed in 1M HCl is rough covered with corrosion products and appeared like full of pits and cavities. This indicated that the inhibitor compounds hinder the dissolution of steel by forming adsorbed layer on the steel surface and there by reduced the corrosion rate.

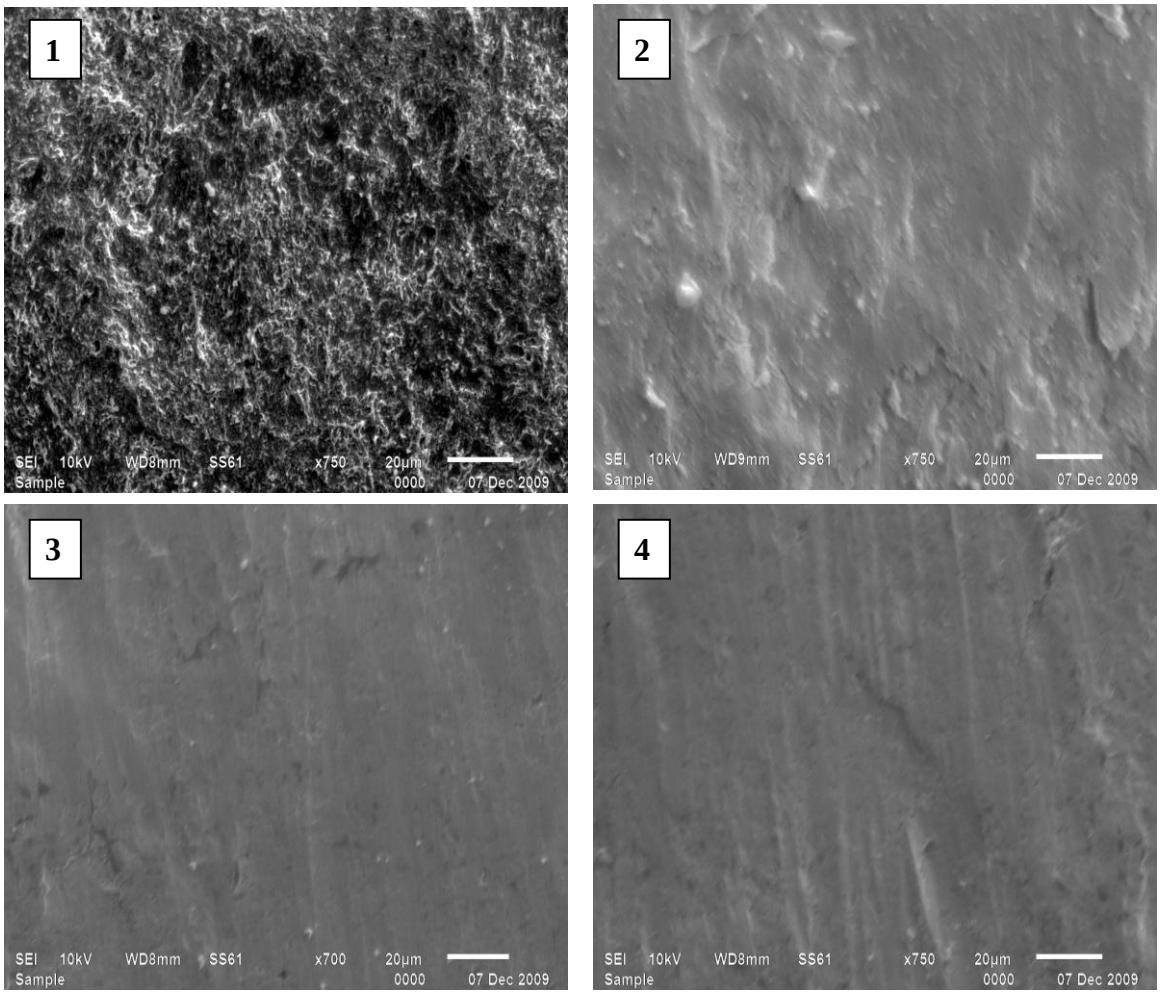

Fig.(3:26): Scanning electron micrographs of the carbon steel surface after 24h immersed at 30^{o}C in (1) 1M HCl, (2) 1M HCl + 5x10^{-3}M compound I, (3) 1M HCl + 5x10^{-3} M compound II and (4) 1M HCl + 5x10^{-3}M compound III.

3.8. Surface active properties

Most organic corrosion inhibitors are adsorbed on the metal/solution interface by displacing water molecules from the surface and forming a compact barrier film. The ability of a surfactant molecule to adsorb is generally directly related to its ability to aggregate and form micelles. There is equilibrium between the singly adsorbed surfactant molecules. The equilibrium occurred at the concentration of complete surface saturation. The micelle formation is the most vital point of view in the surfactant because it is the most effective geometrical arrangement of the molecules at the desired concentration [157]. Below CMC, individual surfactant molecules or monomers tend to adsorb on exposed interfaces, so interfacial aggregation reduces surface tension and is related to corrosion inhibition. The surface tension (γ) of surfactants was measured for a range of concentrations above and below the critical micelle concentration (CMC). A representative plot of γ versus concentration linear decrease in surface tension was observed with the increase of surfactant concentrations [158]. This is a common behavior shown by surfactants in solution and is used to determine their purity and CMC's. The CMC values were obtained from the break point in the γ-log C plots.

3.8.1. Surface tension (γ)

Variation of the surface tension γ values obtained for different concentrations of aqueous solutions of the prepared surfactants is recorded and represented in Fig. (3:27). Sharp decrease in surface tension values is observed as the activity (concentration) increases and then the curves break rather rapidly at still relatively low concentrations and continue to decrease slowly as the concentrations increase.

The critical micelle concentration (CMC) was determined from the intersection points in the γ –log C curves. The obtained CMC values of the synthesized surfactants show a decreasing trend with increasing hydrophobic moiety. This can be accounted for decrease hydration of the hydrophilic part, which favors micellization.

1.8.2. Effectiveness (Π_{CMC})

The effectiveness of the surfactant solution (II_{CMC}) is defined as the difference between the surface tension at the critical micelle concentration (γ_{CMC}) and that for the bi-distilled water (γ_0) at constant temperature [159].

The surface tension values (**γ**) at CMC were used to calculate values of the surface pressure (effectiveness) from equation [160]:

$$\Pi_{CMC} = \gamma_o - \gamma \qquad (3:14)$$

where, γ_o is the surface tension measured for pure water at the appropriate temperature and **γ** is the surface tension at critical micelle concentration. Values of II_{CMC} of the prepared surfactants are listed in Table (3:17). The most effective surfactant is one that gives the greater lowering in surface tension for a critical micelle concentration (CMC). According to the results listed in Table (3:20), compound III, is the most effective surfactant.

1.8.3. Surface excess (Γ_{max})

Maximum surface excess (T_{max}) is defined as the effectiveness of adsorption at an interface. The maximum surface excess concentration of surfactant ions, T_{max}, was calculated from the slope of the straight line in the surface tension plot (dγ/d InC) below CMC, using appropriate form of Gibbs adsorption equation [161,162].

According to Gibb's equation [93]:

$$\Gamma_{max} = -(d\gamma / d \log C)_{\gamma} / (2.303nRT) \qquad (3:15)$$

where, $d\gamma / d \log C$ is the surface pressure, R is the universal gas constant, T is the absolute temperature and value of n is taken as 2 for a dimeric surfactant made up of a divalent surfactant ion and two univalent counterions in the absence of a swamping electrolyte. A substance that lowers the surface energy is thus presents in excess at or near the surface, i.e., when the surface tension decreases with increasing activity of a surfactant. The values of Γ_{max} were calculated and listed in Table (3:17). It is clear that increasing the hydrophobic character of the cationic gemini surfactants shifts Γ_{max} to lower concentrations.

3.8.4. Minimum surface area (A_{min})

The minimum surface area is defined as the area occupied by each molecule in nm^2 at the liquid/air interface. The minimum surface area occupied by each surfactant molecule at the air/water interface (A_{min}) is calculated according to the following equation [93]:

$$A_{min} = 10^{16}/N\,\Gamma_{max} \qquad (3:16)$$

where, Γ_{max} is the maximum surface excess and N is the Avogadro's number.

The minimum area per molecule at the aqueous solution/air interface increases with increasing length of the hydrophobic part. Analysis of data, listed in Table (3:20), indicates that the surface pressure Π_{CMC} of the prepared surfactants decreases with increasing minimum surface area A_{min} of the surfactant molecule.

3.8.5 Conductivity measurements

Specific conductivity (K) measurements were performed for the prepared surfactants at $30^{o}C$ in order to evaluate the CMC and the degree of counter ion dissociation, β. It is well known that the specific conductivity is linearly correlated to the surfactant concentration in both

the premicellar and in the postmicellar regions and the slope in the premicellar region greater than that in the postmicellar region [163]. The intersection point between the two straight lines gives the CMC while the ratio between the slopes of the postmicellar region to that in the premicellar region gives counter ion dissociation.

The relation between specific conductivity and concentration of the synthesized was shown in Fig. (3:28). Values of degree of counter ion dissociation were calculated and listed in Table (3:18).

Results were showed that, for cationic surfactants, the degree of dissociation of surfactants increase by increasing carbon chain length due to the variation in the electronic charge density on the central nitrogen atom, which depends on the positive inductive effect of the alkyl group and bulkiness of cation.

3.8.6 Standard free energy (ΔG_{mic})

In the charged pseudo-phase model of micelle formation, the standard free energy of micelle formation permole of the synthesized surfactant is given by [93]:-

$$\Delta G_{mic} = (2 - \beta)\, RT \ln(CMC) \quad (3:17)$$

where, R is the gas constant, T the temperature and CMC is expressed in the molarity of the surfactant.

Obviously, the standard free energies of micellization for the synthesized surfactants are always negative, indicating that the micellization is a spontaneous process. The free energy change ΔG_{mic} (CH_2) involved in the transfer of a methylene group from an aqueous environment to the interior of the micelle is negative, thus favoring micellization. This is due to the fact that CMC decreases with increasing length of the hydrophobic group; introduction of additional methylene groups induces micellization.

3.9 The relation between corrosion inhibition and surface properties of the prepared surfactants

The greatest reduction of surface tension (effectiveness, Π_{CMC}) was achieved by compound III compared with that obtained by the other two surfactants. This is in good agreement with the inhibition efficiency results achieved by compound III (Tables 3:1–3:9).

$$\Delta G_{ads} = \Delta G_{mic} - (0.6023\,\Gamma_{max}\,A_{min}) \quad (3:18)$$

It seems that the synthesized surfactants favor adsorption rather than micellization. The fact that ΔG_{ads} is more negative compared with the corresponding ΔG_{mic} may be taken as a strong evidence for the more feasibility of the adsorption of the synthesized surfactants. It notes that Γ_{max} of both compound I and compound II lower than Γ_{max} of compound III. On the other hand, A_{min} values of both compound I and compound II are higher than that of compound III considering this one explain why compound III is more effective than compound I and compound II. The high value of Γ_{max} of compound III indicates that more numbers of molecules are adsorbed. This implies close packing of the adsorbed molecules associated with a less area on the metal surface for each molecule thus leading to more electrostatic interaction of the well packed adsorbed layer and more homogenous adsorbed film. All these parameters explain why compound III is the most effective inhibitor.

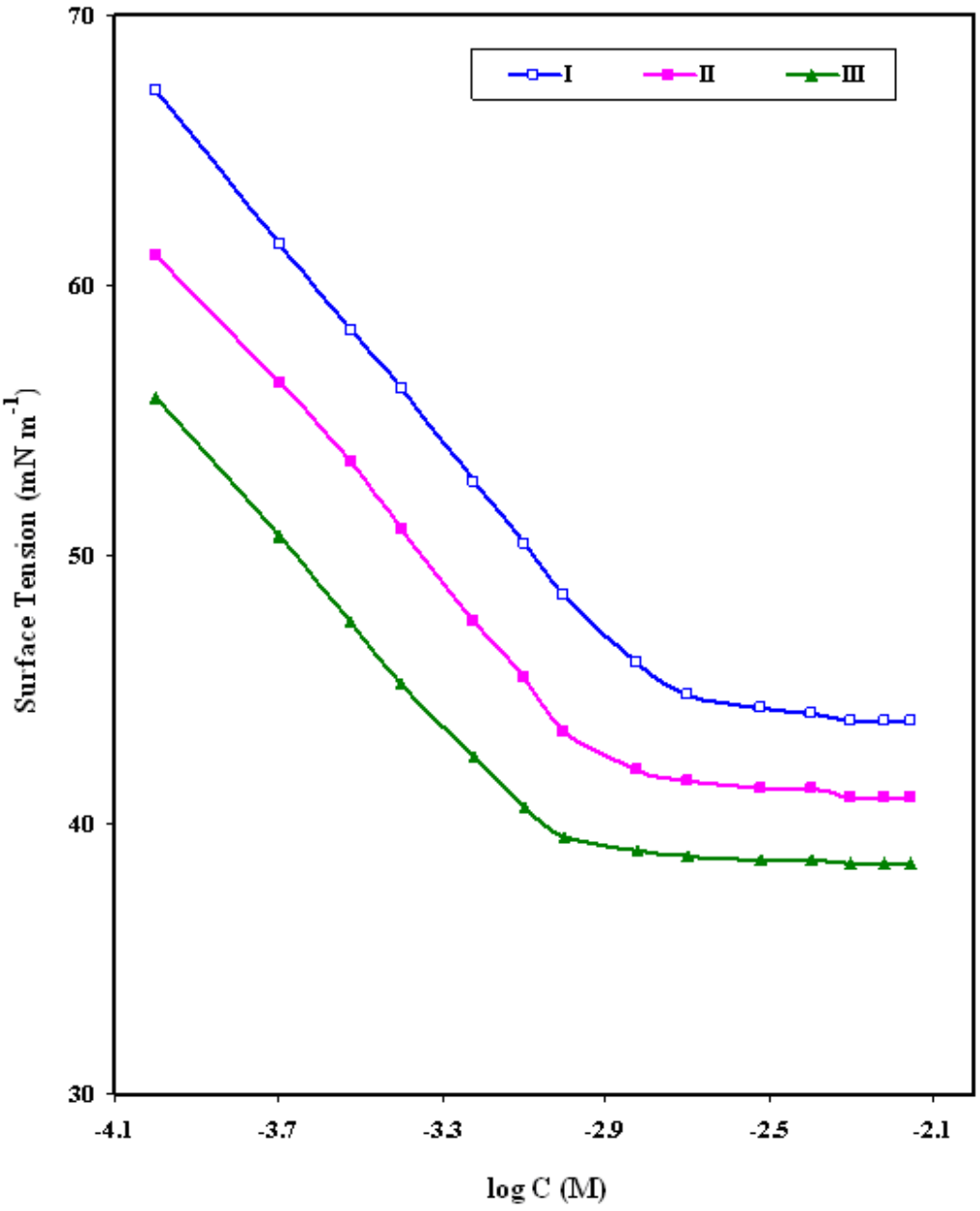

Fig. (3:27): Variation of the surface tension with the synthesized cationic gemini surfactants concentrations in water at 30°C.

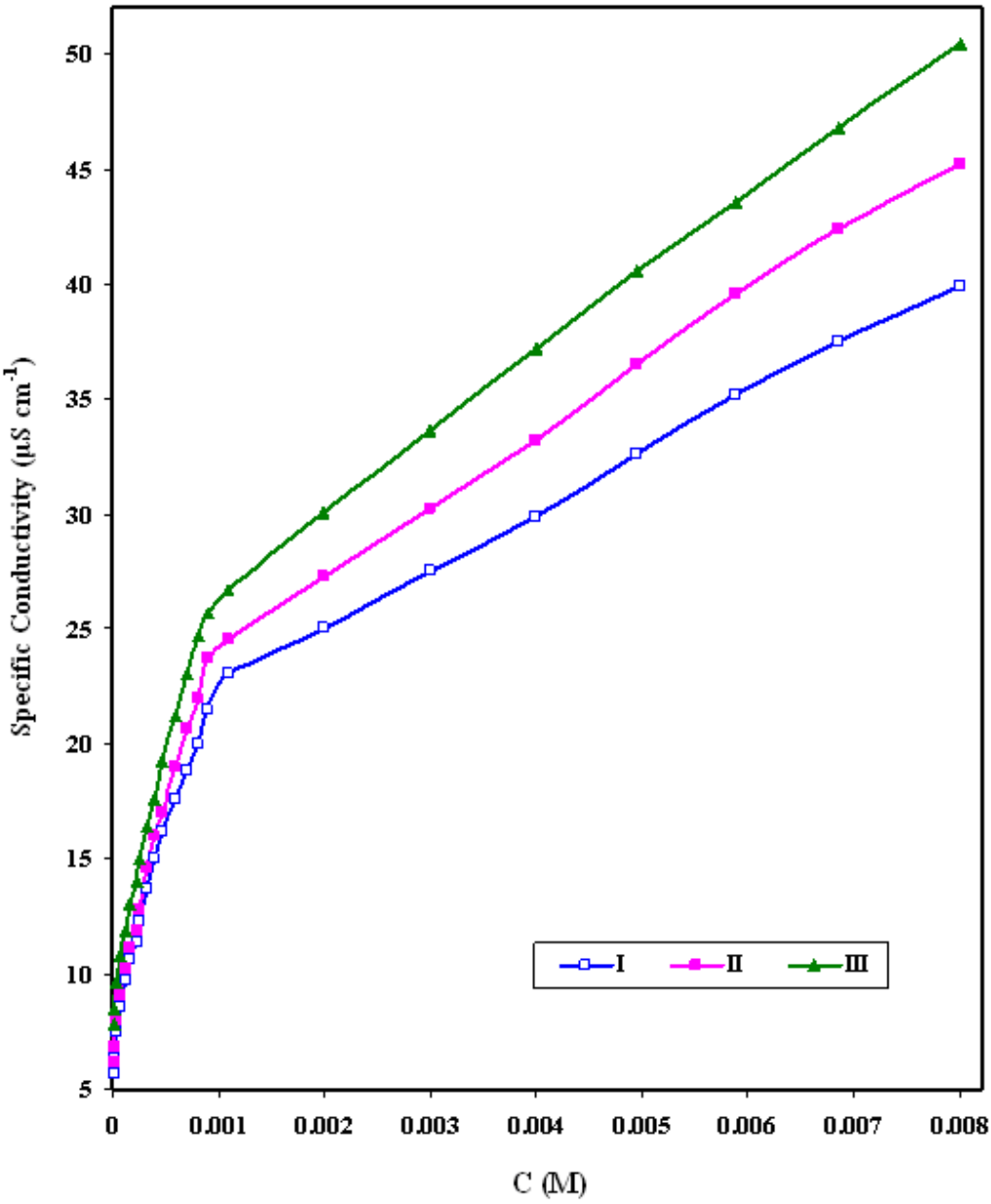

Fig. (3:28): The plots of electrical conductivity against concentration of the synthesized cationic gemini surfactants concentrations in water at 30°C.

Table (3:17): Critical micelle concentration (CMC), effectiveness (Π_{CMC}), maximum surface excess (Γ_{max}), minimum area (A_{min}), and stander free energy ($\Delta G_{mic)}$ of the synthesized cationic gemini surfactants

Inhibitors	CMC x 10^4 (mol dm^{-3})	γ_{CMC} (mN m^{-1})	Π_{CMC} (mN m^{-1})	Γ_{max} x 10^{11} (mol cm^{-2})	A_{min} (nm^2)	ΔG_{mic} kJ mol^{-1}	ΔG_{ads} kJ mol^{-1}
Compound I	12.0	44.9	27.1	10.88	1.53	-30.90	-40.92
Compound II	9.3	42.1	29.9	10.44	1.59	-31.84	-41.83
Compound III	8.0	39.3	32.7	9.92	1.67	-32.26	-42.23

Table (3:18): Critical micelle concentration (CMC) and the degree of counter ion dissociation (β) of the synthesized cationic gemini surfactants

Inhibitors	**CMC x 10^4 (mol dm^{-3})**	**β**
Compound I	**11.0**	**0.146**
Compound II	**9.2**	**0.159**
Compound III	**8.3**	**0.174**